

Article

# Free Surface Energy and Hansen Solubility Parameter Vector Field. Interface Thickness

Rafael Bailón-Moreno \* , Miguel Ángel Bailón-Ruiz and Aqeel Shaikhah Arafat Aljadiri

Departamento de Ingeniería Química, Facultad de Ciencias, Universidad de Granada, Avenida Fuentenueva s/n, 18071 Granada, Spain; miguelangelbailon@gmail.com (M.Á.B.-R.); aqeelalmukhtar@correo.ugr.es (A.S.A.A.)

\* Correspondence: bailonm@ugr.es

**Abstract:** In this paper, a three-dimensional vector field model is proposed, whose dimensions are the Hansen Solubility Parameters: dispersion parameter ( $\delta_D$ ), polarity parameter ( $\delta_P$ ), and hydrogen bonding parameter ( $\delta_H$ ). The vector space that defines the field has the peculiarity of having a dispersion vector with a magnitude of 2 as its base vector, while the polarity and hydrogen bonding vectors have a magnitude of 1. A substance is characterised as a position vector, and the interaction between two substances is determined by calculating the vector difference of both, known as the interaction vector. The interaction among substances may involve solubility, swelling, cracking, surface tension, interface tension, and any physical phenomena where the intermolecular energies of dispersion, polarity or hydrogen bonding come into play. This paper studies free surface energy (surface and interfacial tension). It has been found that free surface energy is directly proportional to the square of the magnitude of the interaction vector. The proportionality constant,  $\tau$ , is expressed in length units, has a value of 0.025 nm, and does not depend on the chemical nature of the substance or state of matter (solid, liquid or gas). The constant value  $\tau$  appears universal and aligns with the thickness of interfaces, thereby supporting Guggenheim's hypothesis. This hypothesis asserts that interfaces possess actual thickness and are not merely mathematical surfaces, as originally postulated by Gibbs. Moreover, it also has been found that the interface thickness,  $\tau$ , is approximately equal to half of the Bohr radius,  $a_0$ , which is defined by universal constants. Because the solubility parameters of thousands of substances are known and can be easily determined from their molecular structure, a good approximation of the surface and interfacial tension of any given substance can now be calculated. It has also been found that the contact angles of sessile droplets in three-phased systems can be calculated from the interaction vectors of the implicated substances.

**Keywords:** Hansen solubility parameters; free surface energy; surface tension; interfacial tension; contact angle; vector field; interaction vector; interface thickness; cohesive energy



**Citation:** Bailón-Moreno, R.; Bailón-Ruiz, M.Á.; Aljadiri, A.S.A. Free Surface Energy and Hansen Solubility Parameter Vector Field. Interface Thickness. *Appl. Sci.* **2024**, *14*, 5834. <https://doi.org/10.3390/app14135834>

Academic Editor: Luca Fiori

Received: 13 June 2024

Revised: 1 July 2024

Accepted: 2 July 2024

Published: 3 July 2024



**Copyright:** © 2024 by the authors. Licensee MDPI, Basel, Switzerland. This article is an open access article distributed under the terms and conditions of the Creative Commons Attribution (CC BY) license (<https://creativecommons.org/licenses/by/4.0/>).

## 1. Introduction

Determining the free surface energy between phases, typically referred to as surface tension in liquid–gas systems and interfacial tension in liquid–liquid systems, is of crucial importance in surface physical chemistry. Many phenomena and applications where free surface energy plays a key role can be cited: the size and shape of liquid droplets or gas bubbles in sprays and foam formation; the formulation of emulsions in cosmetics, food, and other uses; the shape and growth of crystals in industrial crystallizers; capillarity, as in plants where sap rises through xylem vessels; the dispersion and cleaning of surfaces; the formation and properties of nanoparticles influencing catalysis and medicine; hydrophilic and hydrophobic materials for various technical applications like textiles, glass, or paints; oil recovery by surfactant injection; the formulation of high-strength adhesives for industrial and domestic applications; the coating of biomaterials for medical implants; the improved absorption of pesticides and fertilizers in agriculture for greater efficiency and reduced environmental impact; and many more.

The prediction of free surface energy (surface/interfacial tension) and associated properties such as the contact angle or adhesion energy can be achieved using classical methods based on Gibbs thermodynamics formulations. A recent equation in this context is the Shardt–Elliott–Connors–Wright equation [1]. In Gibbs thermodynamics, the free surface energy is accumulated at the interface, which is considered to have zero thickness, and its relative position can be arbitrarily chosen. In contrast, the Kirkwood–Buff equation for surface tensions uses a Gibbsian surface with thickness  $\tau$ , where  $\tau$  is a macroscopic length that is large relative to the range of intermolecular forces [2]. According to these authors, surface tension is proportional to the product of the normal pressure on the interface,  $P$ , and the thickness of the surface,  $\tau$ . For determining pressure, statistical mechanics and molecular density considerations are used, allowing the calculation of surface tension without needing the exact value of  $\tau$ . Another approach is the classical density functional theory [3], where the solid–liquid interfacial tension is obtained as the ratio of the difference in grand potentials of the fluid confined in a slit-like pore and the bulk fluid, and the interface area. These methods generally require molecular parameters, which are often difficult to determine accurately. Furthermore, in Gibbs thermodynamics, the interface is assumed to be a surface with no thickness, which is physically counterintuitive, or if thickness is considered, its size is unknown.

Another alternative extensively researched, although not yet fully satisfactory, is correlating free surface energy with Hansen solubility parameters. This approach will be applied in the present work to establish a general law for evaluating free surface energy (surface/interfacial tension) and contact angles, independent of the chemical nature and physical state of the phases involved. Additionally, the thickness of the interface will be determined. To achieve this, the Hansen solubility parameter space will be reformulated as a vector field.

Prior to this, a brief review of the fundamentals of solubility parameters and an examination of previous attempts to correlate them with free surface energy is necessary.

Hildebrand and Scott suggest that the process of solubilisation is similar to the process of evaporation, as both processes involve the separation of molecules by breaking their intermolecular bonds [4]. To energetically quantify the solubilisation of a substance, Hildebrand defined the solubility parameter,  $\delta$ , as the square root of the cohesive energy density of said substance:

$$\delta = \sqrt{\frac{E}{v}} \quad (1)$$

where  $v$  is the molar volume of the pure substance ( $\text{m}^3/\text{mol}$ ),  $E$  is the energy of vaporization ( $\text{J}/\text{mol}$ ) and  $E/v$  is the cohesive energy ( $\text{J}/\text{m}^3$ ).

Charles M. Hansen considered that the Hildebrand Solubility Parameter is valid when it comes to the global energy balance, but it does not include structural considerations of molecules [5]. That would explain why substances with a similar heat of vaporization and different molecular structures cannot be dissolved between them. To overcome this obstacle, Hansen considers the solubility parameter to be the combination of three solubility parameters:

$$\delta^2 = \delta_D^2 + \delta_P^2 + \delta_H^2 \quad (2)$$

where  $\delta_D$ ,  $\delta_P$  and  $\delta_H$  are the dispersion, polarity, and hydrogen bond solubility parameters, respectively. The “distance”,  $Ra$ , between two substances, called 1 and 2, is determined by the following equation:

$$Ra = \sqrt{4(\delta_{D2} - \delta_{D1})^2 + (\delta_{P2} - \delta_{P1})^2 + (\delta_{H2} - \delta_{H1})^2} \quad (3)$$

The coordinates of each substance are the centre of a sphere with radius  $R_0$ , termed the solubility sphere. Within the solubility sphere, the ‘good solvents’ for the substance are

located, while outside the solubility sphere, the ‘bad solvents’ are found. The parameter called *RED* (Relative Energy Difference) is defined as follows:

$$RED = \frac{Ra}{R_0} \quad (4)$$

When  $RED > 1$ , the substance is not soluble in the considered solvent, while if  $RED \leq 1$ , the opposite will be true.

The Hansen solubility parameters have been related not only to the phenomenon of solubility but to a multitude of phenomena in which surface free energy is involved. Various correlations have been found between surface and interfacial tension,  $\sigma$ , with solubility parameters that respond to the general expressions [4–10]:

$$\sigma = f\left(a\delta_D^\alpha, b\delta_P^\beta, c\delta_H^\gamma, v^d\right) \quad (5)$$

where  $v$  is the molar volume and the constants  $a, b, c, d, \alpha, \beta$  and  $\gamma$  are empirical adjustment constants without physical meaning.

Various correlations between surface and interfacial tension versus the Hansen solubility parameters are shown in Table 1.

**Table 1.** Correlations of surface free energy with solubility parameters.

Equation	Comments	References
$\delta = v^{-2/3}\sigma^{0.5}$	Surface free energy, $\sigma$ ; Hildebrand solubility parameter, $\delta$ ; molar volume, $v$ .	Hildebrand and Scott (1950) [4]
$\sigma = 0.0688v^{1/3} [\delta_D^2 + k(\delta_P^2 + \delta_H^2)]$	$\sigma$ is the surface tension, and $k$ is a constant depending on the liquids involved: 0.8 for several homologous series, 0.265 for normal alcohols, and 10.3 for n-alkyl benzenes.	Skaarup and Hansen (1967), cited in Hansen (2007) [5]
$\delta_D^2 + a\delta_P^2 + b\delta_H^2 = 13.9\left(\frac{1}{v}\right)^{1/3} \sigma$	Hansen solubility parameters, $\delta_D, \delta_P$ , and $\delta_H$ ; molar volume, $v$ ; surface free energy, $\sigma$ . For non-alcohols, $a = b = 0.632$ . For majority of alcohols, $a = 1.000$ and $b = 0.060$ . For acids, phenols, and amines, $a = 2.000$ and $b = 0.481$ .	Beerbower (1971) [6]
$\delta_D^2 + \delta_P^2 = 13.8\left(\frac{1}{v}\right)^{1/3} \sigma$	Like the Beerbower equation, with $a = 1$ and no $\delta_H$ . It adjusts the surface tension of almost all substances well, but not that of some cyclic compounds, acetonitrile, some carboxylic acids and multifunctional alcohols.	Koenhen and Smolders (1975) [7]
$\delta_D^2 = 13.2\left(\frac{1}{v}\right)^{1/3} \sigma_D$	Only used for hydrocarbons without permanent dipoles, and adjusts the dispersion component of the surface tension, $\sigma_D$ .	Koenhen and Smolders (1975) [7]
$\sigma_L = 0.0146(2.28\delta_{DL}^2 + \delta_{PL}^2 + \delta_{HL}^2)v^{1/5}$	Surface tension of 498 pure liquids, $\sigma_L$ , with the solubility parameters and molar volume.	Abbott and Hansen (2013) [11]
$(\delta_D^A - \delta_D^B)^2 + \left(\sqrt{a^A}\delta_P^A - \sqrt{a^B}\delta_P^B\right)^2 + \left(\sqrt{a^A}\delta_H^A - \sqrt{a^B}\delta_H^B\right)^2 = A\left(\frac{2}{v^A + v^B}\right)^{1/3} \sigma_{AB}$	Interfacial tension between two phases, $A$ and $B$ , $\sigma_{AB}$ . $A$ is $0.1 \text{ mol}^{-1}$ . For non-alcohols, $a = b = 0.63$ , and for majority of alcohols $a = 1.000$ and $b = 0.060$ .	Large et al. (2017) [8]
$\frac{\sigma}{[\delta_D + 0.25(\delta_P + \delta_H)]^{1.86}} = 0.68\sigma^{0.82}$ $\sigma = 0.12[\delta_D + 0.25(\delta_P + \delta_H)]^{1.86}$ And other equations.	Does not include molar volume, $v$ . The ratio between $\delta_D$ to $\delta_P$ and $\delta_H$ is 4 to 1.	Neveen AlQasas et al. (2023) [9]

Table 1. Cont.

Equation	Comments	References
$\sigma_{12} = 0.947 \cdot 10^{-8} (\delta_{D1} - \delta_{D2})^2 + 0.314$ $\cdot 10^{-8} (\delta_{P1} - \delta_{P2})^2 + 0.238$ $\cdot 10^{-8} (\delta_{H1} - \delta_{H2})^2$	<p>For two substances, 1 and 2, liquids or solids. When substance 2 is air, because it is a gas, it is assumed that its cohesion energy is very small and <math>\delta_{D2} = \delta_{P2} = \delta_{H2} = 0</math>.</p> <p>Since this can be used with solids and liquids indistinctly, it is possible to approximately evaluate the contact angles for technical applications.</p>	Masakazu Murase et al. [10]

The present work aims to establish, both theoretically and experimentally, a vector field model for the Hansen solubility parameters. This model will allow, in the first place, the characterisation of substances as components of a vector. The coordinates of this vector will be the dispersion ( $\delta_D$ ), polarity ( $\delta_P$ ), and hydrogen bonding ( $\delta_H$ ) parameters of the substances. In the second place, it will enable the evaluation of physical processes and phenomena in which different substances interact as a function of the vectors that characterise these processes, referred to as interaction vectors. The immediate practical applications of the Hansen vector field and interaction vectors are evident in surface processes, where free surface energy is a critical factor, manifesting as surface tension, interfacial tension, and the contact angle.

The hypothesis assumes that the free surface energy is proportional to the square of the magnitude of the interaction vector between the phases involved, where the proportionality constant will have an identifiable physical meaning. This interaction vector, which will be defined later, is closely related to the cohesive energy density.

This hypothesis is very reasonable as it is since free surface energy, which has units in the International System of  $\text{J}/\text{m}^2$ , must be proportional to the cohesive energy density, which has units of  $\text{J}/\text{m}^3$ , where the proportionality constant should be a distance, with the unit being meters.

$$\frac{\text{J}}{\text{m}^2} = m \frac{\text{J}}{\text{m}^3} \quad (6)$$

## 2. Materials and Methods

This work is mainly based on experimental data published on surface tensions, interfacial tensions, and contact angles.

In the case of the surface tensions of liquids, we have also included values that we experimentally determined using the droplet weight method [12]. A perfect concordance has been observed between our values and the ones already published. Additional surface tension data have been published by Masakazu Murase and Daisuke Nakamura in 2023 [10].

The Hansen solubility parameters values used in this study are sourced from the solvents Table A1 and polymers Table A2 in the Appendix A of “Hansen Solubility Parameters. A User’s Handbook” [5]. The free surface energy data of solids with air,  $\sigma_{LG}$ , at 25 °C come from Weiyan Yu and Wanguo Hou, 2019 [13]. The interfacial tension of solids with liquids,  $\sigma_{SL}$ , at 25 °C comes from Masakazu Murase and Daisuke Nakamura, 2023 [10]. The contact angle of diverse liquids over PMMA and n-Octacosane comes from J. Panzer, 1973 [14].

## 3. Data and Discussion

Before delving into specific empirical data and its discussion, the Hansen Solubility Parameters will be reformulated as a vector field. This will enable a more successful approach to the subsequent discussions.

### 3.1. The Hansen Solubility Parameters Vector Field

#### 3.1.1. Concepts and Definitions

Hansen solubility parameters correspond to a three-dimensional vector field in which the dimensions are London dispersion forces,  $D$ , polarity forces due to permanent dipoles,  $P$ , and forces due to hydrogen bonding,  $H$ . The said vector field dictates the physical

phenomena where intermolecular forces (like solubility, polymer swelling and cracking), or free surface energies (surface tension, interfacial tension, contact angle and others) come into play.

Inside that vector field, any given substance is a vector,  $\vec{S}$ , composed of the sum of three vectors:

$$\vec{S} = \vec{S}_D + \vec{S}_P + \vec{S}_H \quad (7)$$

where their components are the multiplication of the scalar solubility parameters by the direction vectors,  $\hat{i}$ ,  $\hat{j}$  and  $\hat{k}$ , of the base of vector space.

$$\vec{S}_D = \delta_D \hat{i} \quad \vec{S}_P = \delta_P \hat{j} \quad \vec{S}_H = \delta_H \hat{k} \quad (8)$$

The particularity of the Hansen vector field is that the magnitude of the direction vectors of the field base,  $\hat{j}$  y  $\hat{k}$ , is 1 (like in Euclidean fields); meanwhile, the magnitude of the vector of the base  $\hat{i}$  is two times bigger. In other words, their magnitudes are as follows:

$$|\hat{i}| = 2 \quad |\hat{j}| = 1 \quad |\hat{k}| = 1 \quad (9)$$

The vector field base is orthogonal.

The vector that represents a substance in the vector field is a position vector and it is expressed as the following:

$$\vec{S} = \delta_D \hat{i} + \delta_P \hat{j} + \delta_H \hat{k} \quad (10)$$

Likewise:

$$\vec{S} = (\delta_D, \delta_P, \delta_H) \quad (11)$$

This vector starts in the origin and has its destination at a certain point of the field  $(\delta_D, \delta_P, \delta_H)$ . The magnitude of vector  $\vec{S}$  is as follows:

$$|\vec{S}| = \sqrt{(\delta_D \hat{i})^2 + (\delta_P \hat{j})^2 + (\delta_H \hat{k})^2} \quad (12)$$

Because  $|\hat{i}| = 2$ , this leads to the following:

$$|\vec{S}| = \sqrt{4\delta_D^2 + \delta_P^2 + \delta_H^2} \quad (13)$$

The coefficient 4 that goes with the dispersion component is obtained by squaring the direction vector  $\hat{i}$ .

Figure 1 shows three substances, namely 1, 2 and 3, with their vectors  $\vec{S}_1$ ,  $\vec{S}_2$  and  $\vec{S}_3$ . It can be observed that, in the base of the space, the direction vector  $\hat{i}$  is twice as large as vectors  $\hat{j}$  and  $\hat{k}$  and, therefore, the scale of  $\delta_D$  is twice the scales of  $\delta_P$  and  $\delta_H$ .

The interaction between substances 1 and 2 is represented by a new vector  $\vec{S}_{12}$  called the interaction vector, which is defined by the difference between both said vectors:

$$\vec{S}_{12} = \vec{S}_2 - \vec{S}_1 \quad (14)$$

$$\vec{S}_{12} = (\delta_{D2} - \delta_{D1})\hat{i} + (\delta_{P2} - \delta_{P1})\hat{j} + (\delta_{H2} - \delta_{H1})\hat{k} \quad (15)$$

Vector  $\vec{S}_{21}$  is directed from 2 to 1. Additionally, it is true that the magnitudes of the interaction vectors  $\vec{S}_{12}$  and  $\vec{S}_{21}$  are idempotent. According to Hansen, these magnitudes correspond to the distance,  $Ra$ , between 1 and 2:

$$|\vec{S}_{12}| = Ra_{1,2} = \sqrt{4(\delta_{D2} - \delta_{D1})^2 + (\delta_{P2} - \delta_{P1})^2 + (\delta_{H2} - \delta_{H1})^2} \tag{16}$$

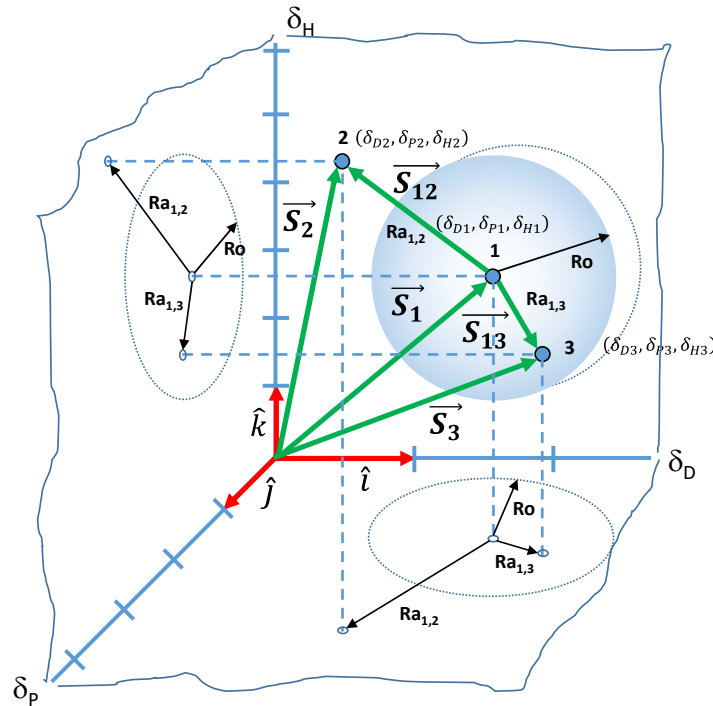


Figure 1. Hansen solubility parameters vector space.

Likewise, the interaction vectors for substances 1 and 3, and substances 2 and 3, are defined as follows:

$$\vec{S}_{13} = \vec{S}_3 - \vec{S}_1 \tag{17}$$

$$\vec{S}_{23} = \vec{S}_3 - \vec{S}_2 \tag{18}$$

The interaction between substances could be referred to as the solubility, swelling, cracking, interfacial tension, or any other physical phenomenon in which any of the intermolecular energies of dispersion, polarity or hydrogen bonding came into play.

Let us consider a case in which the interaction consists of solubilization. In the depicted scenario, as shown in Figure 1, the sphere that surrounds substance 1 represents the volume in which *good solvents* are found. In this illustration, a *good solvent* is substance 2, whereas substance 3, which is out of the solubility sphere, is a *bad solvent*. Therefore,  $RED > 1$  for solvent 2, while  $RED < 1$  for solvent 3.

### 3.1.2. Interaction Vectors and Free Surface Energy

As presented in the introduction above, a great deal of research work has been performed to link free surface energy with the Hansen solubility parameters. In all cases, the  $\delta_D$ ,  $\delta_P$ , and  $\delta_H$  parameters have been conceived as three independent magnitudes with no interdependence whatsoever. To name an example, in the Beerbower equation [6], the

solubility parameters are affected by the  $a$  and  $b$  parameters, which change depending on the chemical family studied.

$$\delta_D^2 + a\delta_P^2 + b\delta_H^2 = 13.9 \left(\frac{1}{v}\right)^{1/3} \sigma \quad (19)$$

In this paper,  $\delta_D$ ,  $\delta_P$ , y  $\delta_H$  will be conceptualised as components of a vector in a vector space. The three-dimensional basis of this space is defined by a director vector, which has a magnitude of 2 for the dispersion forces. In contrast, the magnitudes of the director vectors for polarity and hydrogen bonding forces are set to 1.

Taking the above into account, free surface energy is regarded as directly proportional to the square of the magnitude of the interaction vector between the two phases that create the surface:

$$\sigma_{12} = \tau \left| \vec{S}_{12} \right|^2 \quad (20)$$

That is to say:

$$\sigma_{12} = \tau \left[ 4(\delta_{D2} - \delta_{D1})^2 + (\delta_{P2} - \delta_{P1})^2 + (\delta_{H2} - \delta_{H1})^2 \right] \quad (21)$$

If phase 1 is air, and since its cohesion energy is very weak, the solubility parameters can be considered equal to zero. In this case, the surface free energy (surface tension) would be as follows:

$$\sigma = \tau \left[ 4\delta_D^2 + \delta_P^2 + \delta_H^2 \right] \quad (22)$$

The proportionality constant is called  $\tau$ , and its units are of length.

### 3.2. Surface Tension of Liquids

Surface tension is the interaction between a liquid phase and air or any other gas. It is thought that, because the cohesion energy is very low in gases, their solubility parameters will be negligible:  $\delta_{D,gas} = \delta_{P,gas} = \delta_{H,gas} = 0$ . As such, the interaction vector of a liquid phase with a gas phase will, in general, be as follows:

$$\vec{S}_{LG} = \delta_{DL}\hat{i} + \delta_{PL}\hat{j} + \delta_{HL}\hat{k} \quad (23)$$

Nonetheless, when a liquid interacts with air (which is non-polar), it can present the following behaviours depending on the molecular structure of the liquid (Figure 2), and these will modify the number of dimensions to be considered in the interaction vector:

- (a) The liquid is completely non-polar, and its molecules do not present any special orientation at the interface with air, since its molecules are, like the air molecules, non-polar. The only relevant parameter is  $\delta_D$ , as  $\delta_P = 0$  and  $\delta_H = 0$ . This is the case, for instance, for hydrocarbons like pentane.
- (b) The liquid is polar, but the molecular size is sufficiently large to hide its hydrogen bonds in the inner part of the liquid, preventing them from interacting with air. The electric dipole moment cannot be hidden because it affects the molecule itself. In this case,  $\delta_H$  would not be relevant to the air–liquid interaction, while dispersion and polarity would. Figure 2 shows the example of a carboxylic acid like hexanoic acid. The five-atom carbon chain creates a non-polar barrier that would conceal the hydrogen bonds.
- (c) The liquid is polar, but the molecular size is very small, and non-polar hydrocarbon chains are not able to hide the hydrogen bonding effect versus the air. In this case, the variables of the three solubility parameters, namely dispersion, polarity, and hydrogen bonding, would be relevant. Figure 2 shows the case of formic acid, a small polar molecule with hydrogen bonds that cannot be concealed.

According to the suggested hypothesis, the surface tension will be directly proportional to the magnitude of the interaction vector between the liquid and the gas.

$$\sigma_{LG} = \tau_{LG} \left| \vec{S}_{LG} \right|^2 \quad (24)$$

In cases (a) and (b), the vectors of these molecules would operate in the Hansen vector space governed by dimensions  $D$  and  $P$ , since hydrogen bonding,  $H$ , is non-existent or masked. In this instance, the vector representing these molecules would be two-dimensional:

$$\vec{S}_{LG} = \delta_{DL} \hat{i} + \delta_{PL} \hat{j} \quad (25)$$

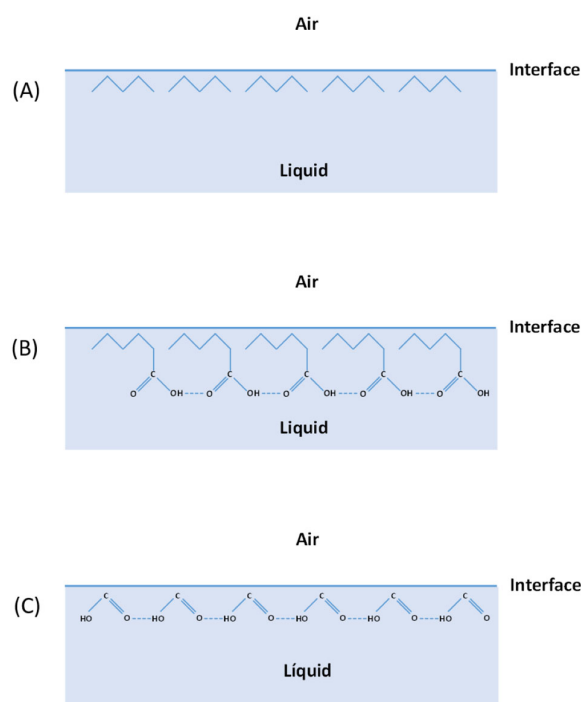


**Figure 2.** Liquid–air interface for (A) pentane, (B) hexanoic acid and (C) formic acid.

Then, according to (24), the surface tension of most liquids (excluding polar ones, such as water, glycols, glycerine, amines, amides, sulfoxides, and low-molar-mass carboxylic acids) can be calculated using the following expression:

$$\sigma_{LG} = \tau_{LG} \left( 4\delta_{DL}^2 + \delta_{PL}^2 \right) \quad (26)$$

In case (c), vectors of the small polar molecules would operate to the full extent of the Hansen vector field governed by dimensions  $D$ ,  $P$ , and  $H$ . In this instance, the vector that represents these molecules would be three-dimensional:

$$\vec{S}_{LG} = \delta_{DL} \hat{i} + \delta_{PL} \hat{j} + \delta_{HL} \hat{k} \quad (27)$$

Then, according to (24), the surface tension of polar liquids, including water, glycols, amines, amides, sulfoxides, and low-molar-mass carboxylic acids, can be calculated using the following:

$$\sigma_{LG} = \tau_{LG} \left( 4\delta_{DL}^2 + \delta_{PL}^2 + \delta_{HL}^2 \right) \quad (28)$$

To prove these hypotheses, the surface tension data of 122 liquids and values measured by the authors using the droplet weight method [12] have been gathered and analyzed.

### 3.2.1. Surface Tension of Non-Polar Liquids or Polar with Non-Small Molecular Size as Function of the Interaction Vector

Table A1, in Appendix A, shows the surface tension and Hansen solubility parameter data for liquids of very diverse chemical categories such as aliphatic hydrocarbons, cyclic hydrocarbons, aromatic compounds, chlorinated derivatives, alcohols, ketones, carboxylic acids, esters, ethers, glycol ethers, nitrogen compounds, etc. They all are liquids included in the above-mentioned cases (a) and (b) and represent most liquids. In Figure 3, the surface tension versus the square of the interaction vector magnitude and the linear regression for these compounds are shown. The correlation is excellent as a fitting coefficient  $R^2 = 0.990$ . The standard deviation of the absolute errors of the surface tension is 3.2 mN/m, and the mean is 2.9 mN/m.

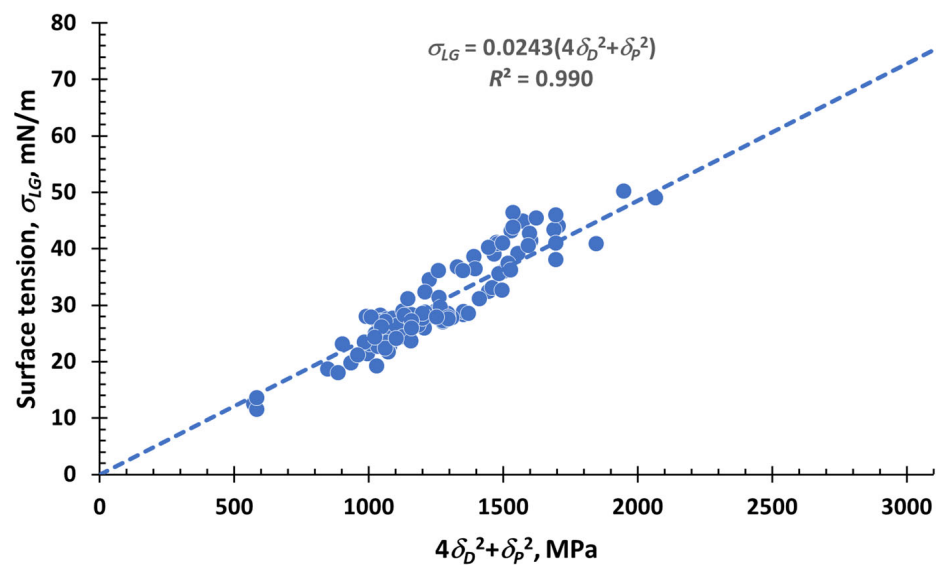


**Figure 3.** Correlation of surface tension,  $\sigma_{LG}$ , and  $4\delta_D^2 + \delta_P^2$ , for every molecule type except for low-molecular-mass polar molecules.

It is proven that in this case, the surface tension is directly proportional to the square of the magnitude of the interaction vector, with the following expression:

$$\sigma_{LG} = 0.0243(4\delta_{DL}^2 + \delta_{PL}^2) \quad (29)$$

Generalizing:

$$\sigma_{LG} = 0.0243 \left| \vec{S}_{LG} \right|^2 \quad (30)$$

where the surface tension,  $\sigma_{LG}$ , is expressed in mN/m, the vector magnitude is expressed in MPa and  $\tau_{LG} = 0.0243$  nm. It is worth noting that  $\tau_{LG}$  does not depend on the molar volume and its units are those of length.

The equation of a circle with its origin as the center of a plane is as follows:

$$x^2 + y^2 = R^2 \quad (31)$$

where  $x$  and  $y$  are abscissa and ordinate axis coordinates, respectively, and  $R$  is the radius of the circle. If (29) is reorganized, it is found that it also fits the equation of a circle with its center as the origin of coordinates within the Hansen  $DP$  plane:

$$4\delta_{DL}^2 + \delta_{PL}^2 = 41\sigma_{LG} \quad (32)$$

The abscissa, being in a Hansen vectorial field, is multiplied by 2 (4 when squared), and the radius circle,  $R_\sigma$ , is as follows:

$$R_\sigma = \sqrt{41\sigma_{LG}} \quad (33)$$

This expression allows us to draw lines of equal tension (iso-tension lines) in a  $DP$  diagram. Knowing the solubility parameters  $\delta_D$  and  $\delta_P$  of any given liquid (except for low molar mass, polar ones), its surface tension can be graphically determined with ease (Figure 4).

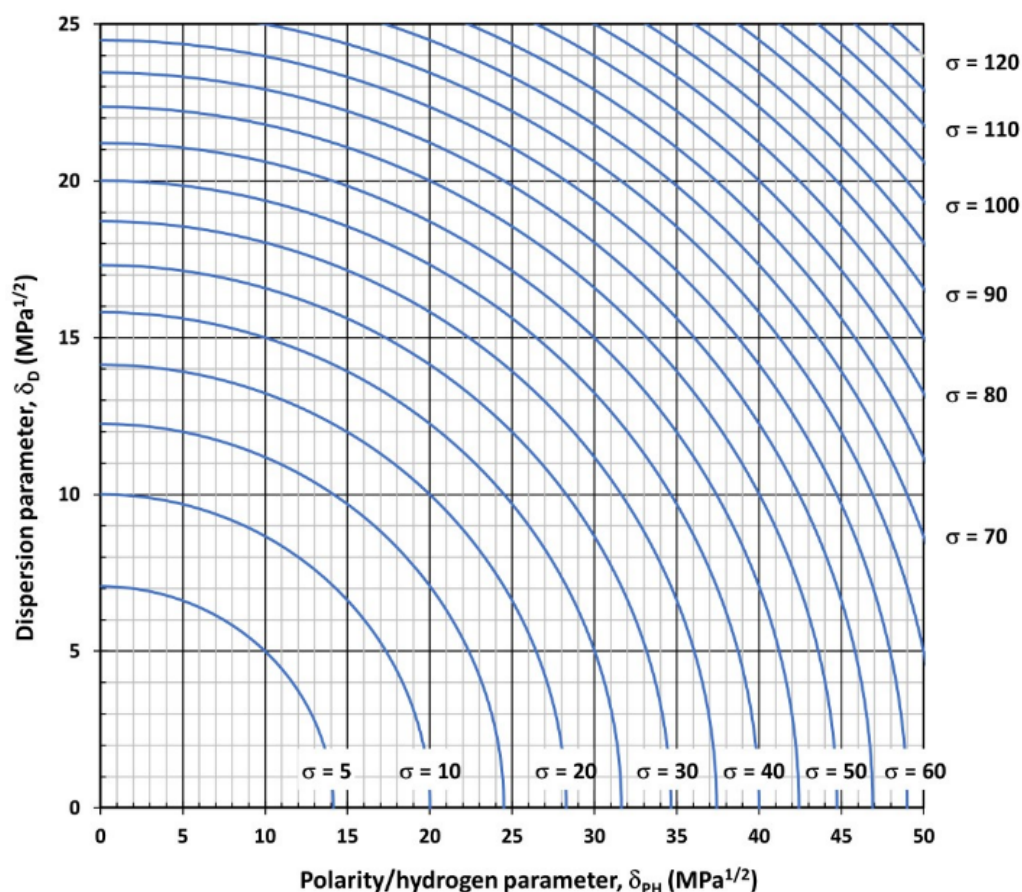


**Figure 4.** Surface Iso-tension curves,  $\sigma$ , in mN/m for liquid substances with a molar volume,  $v$ , equal to or bigger than  $100 \text{ cm}^3/\text{mol}$  for every hydrogen bonding parameter value,  $\delta_H$ .

### 3.2.2. Surface Tension of Polar or Non-Polar Liquids with Not-Small Molecular Size as Function of the Interaction Vector

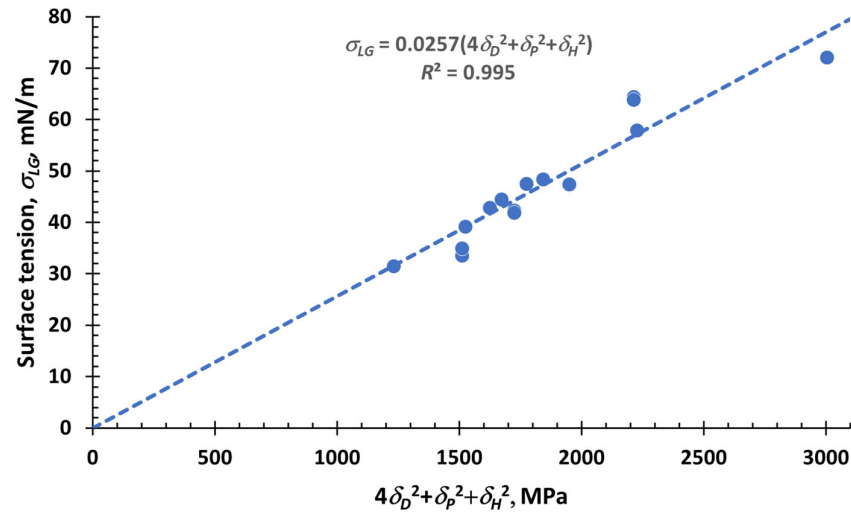
Table A2, in Appendix A, shows the surface tension data of small polar molecules including water, glycols, glycerine, nitrogen compounds and dimethyl sulfoxide. Their molecules are small and cannot hide their hydrogen bonds from air, which is why the interaction vector operates in the entire Hansen space volume. The case of 1,5-Pentanediol is not an anomaly: although its molecule is not small, it has a double bond that prevents rotation around the molecule's axis, making the hydroxyl groups difficult to hide. Similarly, a similar situation occurs with 3-hydroxymethylpyridine, a flat, rigid molecule that also does not allow the reorientation of polar substituents. The square of the magnitude of the interaction vector has been calculated by including the three solubility parameters:  $4\delta_D^2 + \delta_P^2 + \delta_H^2$ .

Figure 5 shows surface tension versus the square of the magnitude of the interaction vector, along with the linear regression. The fitting is also excellent, with a coefficient of

$R^2 = 0.995$ . The standard deviation of the absolute errors of the surface tension is 3.7 mN/m, and the mean is 3.0 mN/m.

For the case of small polar molecules, it is also correct that the surface tension is directly proportional to the square of the module of the interaction vector that encompasses the entire Hansen vector space. It is further demonstrated that, in this instance, the surface tension is directly proportional to the square of the interaction vector according to this expression:

$$\sigma_{LG} = 0.0257(4\delta_{DL}^2 + \delta_{PL}^2 + \delta_{HL}^2) \tag{34}$$



**Figure 5.** Correlation between surface tension,  $\sigma_{LG}$ , and  $4\delta_D^2 + \delta_P^2 + \delta_H^2$  for polar and low-mass molecules.

And generalizing:

$$\sigma_{LG} = 0.0257 \left| \vec{S}_{LG} \right|^2 \tag{35}$$

The surface tension,  $\sigma_{LG}$ , is expressed in mN/m, the units of the vector magnitude are MPa, and  $\tau_{LG} = 0.0257$  nm, being very similar to the value obtained for non-small molecules. As such,  $\tau_{LG}$  is independent of the molar volume and polarity, regardless of the molecular size.

The equation of a sphere with the origin as its center is given by the following expression:

$$x^2 + y^2 + z^2 = R^2 \tag{36}$$

where  $x, y, z$  are the coordinates of the three axes of the space, and  $R$  is the radius of the sphere. If Equation (34) is reorganized, it is found that it also fits the equation of a sphere with the origin of coordinates as its center in the Hansen vector field:

$$4\delta_{DL}^2 + \delta_{PL}^2 + \delta_{HL}^2 = 39\sigma_{LG} \tag{37}$$

The abscissa, being in a Hansen vectorial field, is multiplied by 2 (4 when squared), and the radius of the circle is  $R_\sigma$ :

$$R_\sigma = \sqrt{39\sigma_{LG}} \tag{38}$$

It should be noted that surface tension spheres resemble the well-known Hansen solubility spheres. This shows that surface tension is a phenomenon closely related to solubilization: dispersion, polarity, and hydrogen bonding forces operate in both cases.

### 3.3. Surface Free Energy of Solids

The surface tension of a solid, commonly known as surface free energy, is the result of the interaction of a solid with air or any other gas. Because the cohesion energy of gases is negligible, their solubility parameters will be zero, or, in other words  $\delta_{D,gas} = \delta_{P,gas} = \delta_{H,gas} = 0$ . Unlike liquids, in which molecules have mobility and can reorient themselves when interacting with a gas to show their least ionised part at the liquid–gas interface, solids cannot do that due to their limited mobility. For this reason, the interaction vector will comprise the following three components: dispersion, polarity, and hydrogen bonding.

$$\vec{S}_{SG} = \delta_{DS}\hat{i} + \delta_{PS}\hat{j} + \delta_{HS}\hat{k} \tag{39}$$

Therefore:

$$\sigma_{SG} = \tau_{SG} \left| \vec{S}_{SG} \right|^2 \tag{40}$$

And:

$$\sigma_{SG} = \tau_{SG} \left[ 4\delta_{DS}^2 + \delta_{PS}^2 + \delta_{HS}^2 \right] \tag{41}$$

Table A3 in Appendix A shows the surface free energy data of 21 solid materials with different degrees of polarity. Additionally, the interaction vector values and calculated free energy data are displayed.

Figure 6 graphically shows the surface tensions (free surface energies) of the solids included in Table A3 in Appendix A and their linear regression. The correlation is satisfactory as  $R^2 = 0.9828$ , despite the difficulty of accurately determining the experimental values of the free surface energies of solids. The constant,  $\tau_{SG} = 0.0260$  nm, is very similar to the values of liquid surface tensions ( $\tau_{LG} \approx 0.0243$  nm  $\approx$  0.0257 nm).

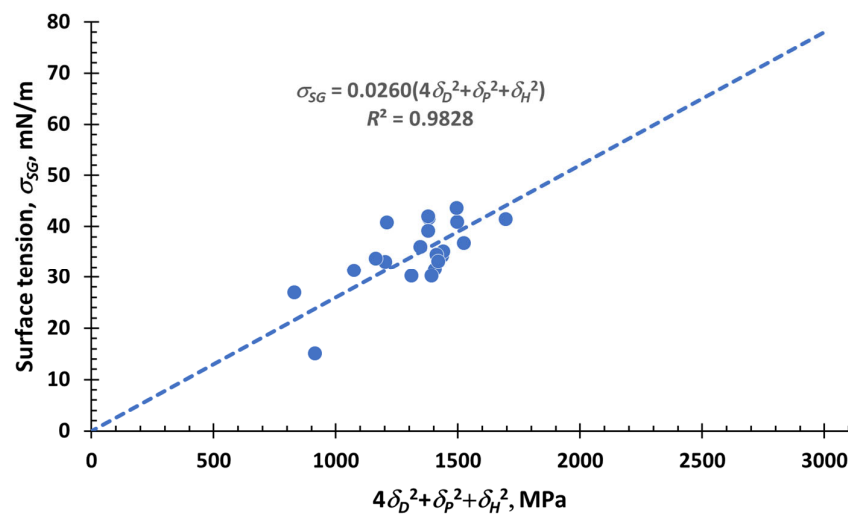


**Figure 6.** Correlation between the surface free energy of solids,  $\sigma_{SG}$ , and  $4\delta_D^2 + \delta_P^2 + \delta_H^2$ .

### 3.4. Interfacial Tension between a Solid and a Liquid, or Any Given Two Substances

The diagram of Figure 7 displays a ternary system comprising a solid (S), a liquid (L) and a gas (G). The following is true:

$$\vec{S}_{SG} + \vec{S}_{SL} = \vec{S}_{LG} \tag{42}$$

The interaction vector between the solid and liquid,  $\vec{S}_{SL}$ , will then be as follows:

$$\vec{S}_{SL} = \vec{S}_{LG} - \vec{S}_{SG} \tag{43}$$



Table A4 shows the experimental interfacial tension data of several liquids with a few solids: polystyrene polymers (PS), polymethylmethacrylate (PMMA), Polyamide 6,6 (PA66), polytetrafluoroethylene (PTFE), and polyvinylbutyral (PVB). The solubility parameters of polymers and various liquids, the square of the module of the interaction vector  $\vec{S}_{SL}$  and the interfacial tension calculated according to (49) are also shown.

The interfacial tensions between solid polymers and liquids and the linear regression are displayed in Figure 8:

$$\sigma_{SL} = 0.0268 \left[ 4(\delta_{DL} - \delta_{DS})^2 + (\delta_{PL} - \delta_{PS})^2 + (\delta_{HL} - \delta_{HS})^2 \right] \quad (50)$$

The value  $\tau_{SL} = 0.0268 \text{ nm}$  is also very similar to previous values found for liquid–gas and solid–gas interactions.

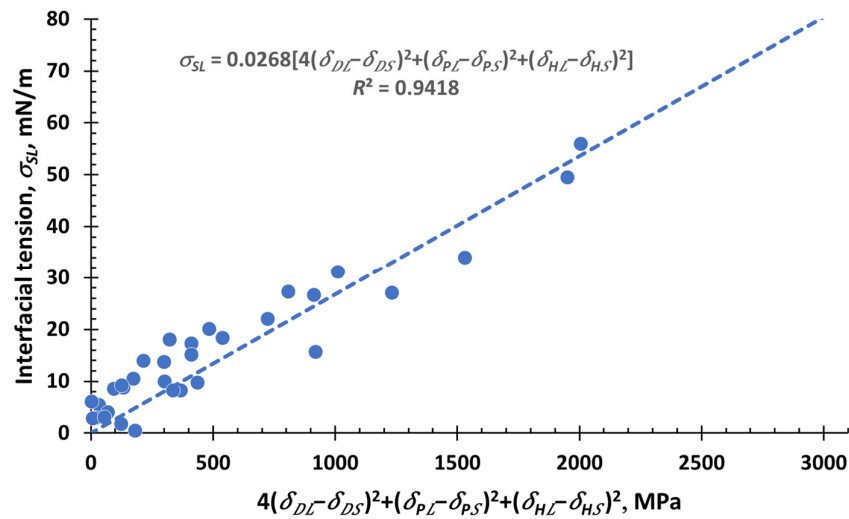


Figure 8. Correlation between interfacial tension of solids with liquids,  $\sigma_{SL}$ , and the square of the module of the interaction vector.

The previous solid–liquid interaction equations can also be extended to the interaction between two liquids. Therefore, for a liquid L1 and a liquid L2, the following can be expressed:

$$\sigma_{L1,L2} = t_{L1,L2} \left| \vec{S}_{L1,L2} \right|^2 = \tau_{L1,L2} Ra^2 \quad (51)$$

$$\sigma_{L1,L2} = \tau_{L1,L2} \left[ 4(\delta_{DL2} - \delta_{DL1})^2 + (\delta_{PL2} - \delta_{PL1})^2 + (\delta_{HL2} - \delta_{HL1})^2 \right] \quad (52)$$

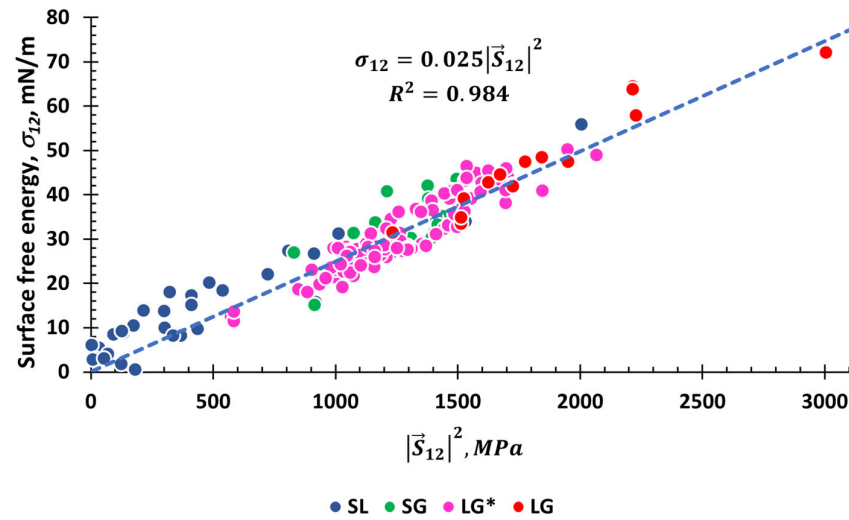
### 3.5. Free Surface Energy: General Equation

Figure 9 plots the surface free energy against the square of the modulus of the interaction vector for liquid–gas interactions (large nonpolar and polar molecules,  $LG$ , and small polar molecules,  $LG^*$ ), solid–gas interactions ( $SG$ ), and solid–liquid ( $SL$ ) interactions. The linear fit for all values is of high quality, since all types of molecules, large and small, polarized and non-polarized, solid, liquid, or gaseous, are correlated.

All of this means that the following expression can be established as a general equation for the evaluation of free surface energy between two substances:

$$\sigma_{12} = \tau \left| \vec{S}_{12} \right|^2 \quad (53)$$

where  $\tau$  is a general constant ( $\tau = 0.025 \text{ nm} = 25 \cdot 10^{-12} \text{ m}$ ) and  $\left| \vec{S}_{12} \right|^2$  is the square of the magnitude of the interaction vector between substance 1 and 2.



**Figure 9.** Correlation between free surface energy and the square of the magnitude of the interaction vector.

For most liquid–gas interactions, except for those involving low-molecular-mass polarized ones, the interactions occur in the *DP* plane:

$$\left| \vec{S}_L \right|^2 = 4\delta_{DL}^2 + \delta_{PL}^2 \tag{54}$$

In the case of high-molecular-mass liquids, the interaction vector operates exclusively in the *DP* plane.

For polarized low-molecular-mass liquids, the entire Hansen field (*DPH* space) is used:

$$\left| \vec{S}_L \right|^2 = 4\delta_{DL}^2 + \delta_{PL}^2 + \delta_{HL}^2 \tag{55}$$

For solid–gas interactions, the *DPH* space is used, too:

$$\left| \vec{S}_S \right|^2 = 4\delta_{DS}^2 + \delta_{PS}^2 + \delta_{HS}^2 \tag{56}$$

For the interaction of any given substance 1 with any given substance 2:

$$\left| \vec{S}_{12} \right|^2 = 4(\delta_{D2} - \delta_{D1})^2 + (\delta_{P2} - \delta_{P1})^2 + (\delta_{H2} - \delta_{H1})^2 \tag{57}$$

If substance 1 or 2 is a gas, this general expression is then transformed into (55) and (56).

### 3.6. Physical Meaning of $\tau$ Constant

Classical approaches to interface thermodynamics, according to Gibbs, involve conceiving interfaces as per their mathematical definition; in other words, these are structures with no volume, only area [15]. Each extensive property of the system, such as free energy, entropy, or the quantity of matter, is divided into three contributions. The first contribution is to a bulk phase in which it is assumed that said extensive property is homogeneous until reaching the maximum mathematical surface. The second is a similar contribution in

the other homogeneous bulk phase, and the third is formed by residues of the extensive property that get assigned to the mathematical surface. That is to say, extensive properties like free energy or entropy get assigned to the mathematical surface but do not get assigned to volume. From a mathematical point of view, this assumption could be valid; however, from a physical perspective, it does not make sense that something without volume could store free energy or entropy. Another obstacle that these approximations face is that the no-volume mathematical surface can be spatially situated at will, allowing selected extensive properties to have an arbitrarily chosen value, including zero.

It must be accepted that the mathematical surface, which by definition does not have volume, does not correspond to the physical representation of an interfacial layer. These objections were manifested by Guggenheim, who proposes a new approach in which interfaces are not a mathematical construct, but a real physical layer with volume and thickness [16]. Guggenheim uses theoretical reasoning to develop the thermodynamics of interfaces in systems formed by various compounds; this comes from the physical existence of the interfacial layer with a thickness estimated to be less than 10 nm, and he does not propose any experimental value.

Dadashev et al. have theoretically studied adsorption in binary systems of indium–tin, gallium–bismuth, and thallium–bismuth. Their aim was to determine the influence of the concentrations of the components on the distance between different positions of an interfacial surface defined according to Gibbs [17]. The obtained equations predict that the said surface must be in a range that would correspond to a physical layer with a thickness smaller than the size of an atom or, in other words, less than 0.1 nm.

It has been proposed that the pressure coefficient, which is a derivative of the interfacial tension with respect to pressure, can be used as a measurement of the interfacial layer thickness,  $\tau$ :

$$\tau = \frac{\partial \sigma}{\partial P} \quad (58)$$

The pressure coefficient, defined as the interfacial tension divided by pressure, has units of distance and is thus a suitable candidate for determining the thickness of an interfacial layer. As such, it has been considered for a long time. However, recently, Junhan Cho et al. studied compressible polymer mixtures and found that, while this coefficient presents values compatible with a potential interfacial layer, it can exhibit negative values in some regions, rendering it incompatible with thickness [18]. They suggest that pressure by itself cannot predict thickness because the interfacial tension is also strongly dependent on the Flory–Huggins theory of the polymer solution interaction parameter,  $\chi_{12}$ . In addition, there is also a dependence on the density of polymer packing,  $\eta$  [19]. In a Monte Carlo simulation about capillary waves in homopolymer interfaces, proportionality between interfacial tension and  $\chi_{12}$  parameter has been found [20].

The polymer–solvent interaction parameter,  $\chi_{12}$ , is defined as follows:

$$\chi_{12} = \frac{z\Delta w}{kT} \quad (59)$$

where  $z$  is the coordination number (number of neighbor units occupied by either a polymer segment or a solvent molecule),  $\Delta w$  is the energy increment because of the interaction between the substance and solvent,  $k$  is the Boltzmann constant, and  $T$  is the absolute temperature. The interaction parameter can be estimated using the following expression [5]:

$$\chi_{12} = \frac{v(\delta_1 - \delta_2)^2}{RT} + \beta \quad (60)$$

where  $v$  is the molar volume of the solvent,  $\delta_1$  is the Hildebrand solubility parameter of the solvent,  $\delta_2$  is the Hildebrand solubility parameter of the polymer,  $R$  is the gas constant and  $T$  is the absolute temperature. The empirical constant,  $\beta$ , is used as a correction for Flory

combinatorial entropy. If the Hansen solubility parameters are considered,  $\chi_{12}$  can also be estimated using the following expression:

$$\chi_{12} = \frac{vA_{12}}{RT} \quad (61)$$

where  $A_{12}$  is as follows:

$$A_{12} = (\delta_{D2} - \delta_{D1})^2 + 0.25(\delta_{P2} - \delta_{P1})^2 + 0.25(\delta_{H2} - \delta_{H1})^2 \quad (62)$$

It can be observed that for an interaction between polymer 2 with solvent 1,  $A_{12}$  is equal to quarter of the square of the interaction vector magnitude  $\vec{S}_{12}$  according to the vector field model:

$$A_{12} = \frac{1}{4} \left| \vec{S}_{12} \right|^2 \quad (63)$$

For this reason,  $\left| \vec{S}_{12} \right|^2$  is proportional to  $\chi_{12}$ :

$$\left| \vec{S}_{12} \right|^2 = \frac{4RT}{v} \chi_{12} \quad (64)$$

By solving (53), the following is obtained:

$$\tau = \frac{\sigma_{12}}{\left| \vec{S}_{12} \right|^2} \quad (65)$$

If we compare this equation with the pressure coefficient in (58), it can be observed that it is also a free surface energy divided by an equivalent pressure magnitude, so the units will be of length. Pressure by itself, as suggested by Junhan Cho [18,19], is not enough to exactly represent the thickness of the interface because, in some way or another, it must contain the parameter  $\chi_{12}$  in its formulation.

Actually,  $\left| \vec{S}_{12} \right|^2$  is a magnitude with pressure as units (a mandatory condition) that is also related to the  $\chi_{12}$  parameter. Therefore, it can be concluded that the expression in (65) represents the thickness of the interface.

When fitting the data by regression, it has been found that  $\tau$  is very close to 0.025 nm in all instances. In other words, it is less than 0.1 nm, just like Dadashev and collaborators predicted [17]. The thickness is smaller than an atom's diameter, and it must be so. Otherwise, the interface would be occupied by the atoms and molecules of one of the phases. The interface can also be visualized as a zone in which the atomic and molecular orbitals of both phases get close but do not belong to either of them, acting a transition between them.

The obtained value  $\tau$  is independent of whether it represents surface or interfacial tension, the chemical family of the substances involved, or the state of matter, whether solid, liquid, or gas. This leads to the conclusion that  $\tau$  is a dimensional characteristic of the interface by itself, rather than being dependent on the nature of the phases.

It could be due to chance or an unknown causal relationship, but the interface thickness,  $\tau$ , is approximately (and with great accuracy) half of the Bohr radius,  $a_0 = 0.05292$  nm.

$$\tau \approx \frac{1}{2} a_0 \quad (66)$$

The Bohr radius is the radius of the orbit of the electron of the hydrogen atom in the atomic model developed by Niels Bohr in 1913 for the quantum number  $n = 1$ . According to the Schrödinger model, the Bohr radius is actually the distance to the nucleus at which

the probability of finding the electron is maximum for the 1s atomic orbital of the hydrogen atom. The radius is obtained from the universal physical constants:

$$a_0 = \frac{2\epsilon_0 h}{m_e e} \tag{67}$$

where  $\epsilon_0$  is the permittivity of the vacuum,  $h$  is the Planck constant,  $m_e$  is the resting electron, and  $e$  is the elemental electric charge.

If there were an unknown but plausible causal relationship, the interface thickness would be a property of the quantum nature resulting from the combination of universal physical constants, and it would follow the next expression:

$$\tau = \frac{\epsilon_0 h}{m_e e} = 0.02646 \text{ nm} \tag{68}$$

Figure 10 shows an idealized representation of an interface located between two molecular monolayers. This interface is the boundary at which the properties of phase 1, especially its solubility parameters,  $\delta_{D1}$ ,  $\delta_{P1}$  and  $\delta_{H1}$ , gradually become the values of phase 2 ( $\delta_{D2}$ ,  $\delta_{P2}$  and  $\delta_{H2}$ ). In this case, the thickness  $\tau$  could also be expressed as the interfacial tension versus the variation in the square of the interaction vector magnitude:

$$\tau = \frac{d\sigma_{12}}{d\left(\left|\vec{S}_{12}\right|^2\right)} \tag{69}$$

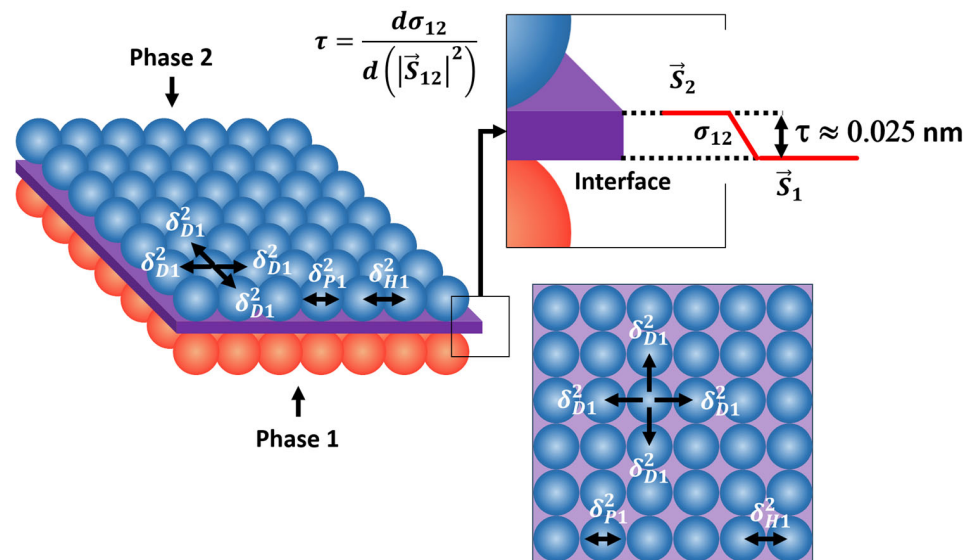


Figure 10. Idealized image of an interfacial layer between two phases.

Figure 10 also shows that the coordination number of molecules from monolayers in contact with the interface is usually four. This implies that the electronic dispersion of a molecule affects four neighboring molecules. For this reason,  $\delta_D^2$  parameter needs to be considered four times. However, the polarity and hydrogen bonding are unidirectional, and thus should only be accounted for once. This is the molecular justification for why dispersion is assessed four times when calculating the magnitude of the interaction vectors. For two (1 and 2) phases:

$$\tau = \frac{\sigma_{12}}{4(\delta_{D2} - \delta_{D1})^2 + (\delta_{P2} - \delta_{P1})^2 + (\delta_{H2} - \delta_{H1})^2} \approx 0.025 \text{ nm} \approx \frac{1}{2} a_0 \tag{70}$$

### 3.7. Contact Angle and the Solubility Parameters Vector Field

The tensions that come into play when a liquid droplet is dropped over a solid surface are shown in Figure 11. The surface tension of the droplet versus air (or any given gas) is  $\sigma_{LG}$ , the surface tension of the solid surface versus air is  $\sigma_{SG}$ , and the interfacial tension between the solid surface and the liquid droplet is  $\sigma_{SL}$ . The tension  $\sigma_{LG}$  is tangent to the surface of the droplet where the three phases come into contact. The angle formed by  $\sigma_{LG}$  is called the contact angle,  $\theta$ .

The cosine of the contact angle is as follows:

$$\cos\theta = \frac{\sigma_{SG} - \sigma_{SL}}{\sigma_{LG}} \tag{71}$$

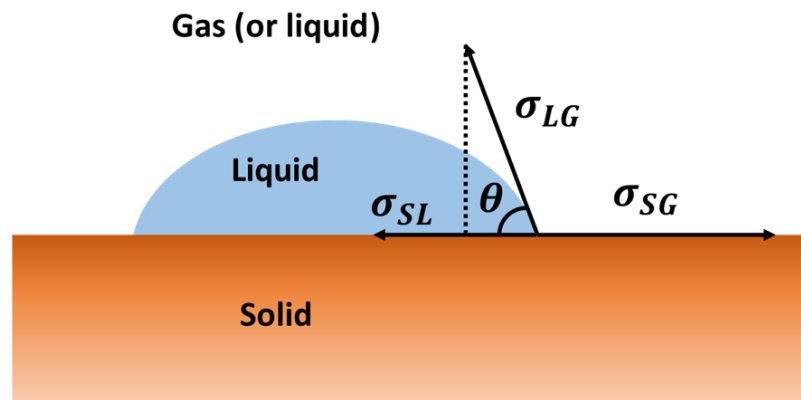


Figure 11. The tension balance of a liquid droplet dropped over a solid surface.

By substituting free surface energies with their expression as a function of the interaction vector it results in, the following is obtained:

$$\cos\theta = \frac{|\vec{S}_{SG}|^2 - |\vec{S}_{SL}|^2}{|\vec{S}_{LG}|^2} \tag{72}$$

Or, in other words:

$$\theta = \arccos\left(\frac{|\vec{S}_{SG}|^2 - |\vec{S}_{SL}|^2}{|\vec{S}_{LG}|^2}\right) \tag{73}$$

If:

$$|\vec{S}_{SG}|^2 - |\vec{S}_{SL}|^2 > |\vec{S}_{LG}|^2 \tag{74}$$

This means that the critical surface tension,  $\sigma_c$ , has been surpassed and values  $\cos\theta = 1$  and  $\theta = 0$  will be directly assigned.

To confirm the validity of (72) and (73), the calculated values have been compared with the experimental values for the contact angles of various liquids on Poly(methyl methacrylate) (PMMA) and n-Octacosane surfaces (Table A5 in Appendix A). Figure 12 shows the correlation between the experimental and calculated values. Experimental contact angle estimation is usually not very accurate because a variety of factors like surface roughness or impurities can distort the measurement. Even so, for the same solid–liquid–gas system, there can be a wide range of contact angles. Within that range of possible contact angles, the largest is called the advancing contact angle and the smallest is known as the

receding contact angle. Despite potential experimental contact angle inconveniences, and the fact that small solubility parameter biases can be amplified when squaring parameters, the correlation can be classified as excellent:  $R^2 = 0.981$ .

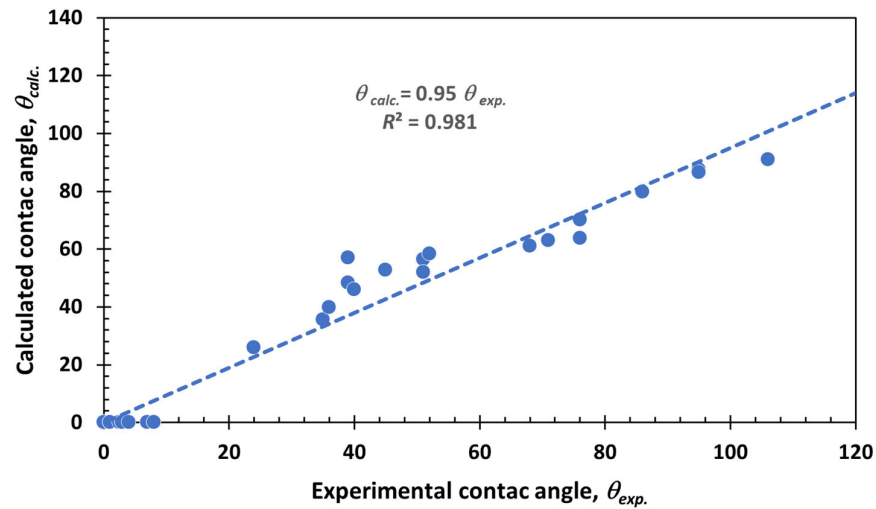


Figure 12. Calculated contact angle versus experimental contact angle.

### 3.8. Contact Angle and Interaction Vectors Angle

Contact angles and interaction vector angles work in two different vector spaces, but they can be linked. Figure 13 depicts an image comparing between the interaction vector angles in the Hansen field,  $\alpha, \beta, \gamma$ , and the contact angle,  $\theta$ .

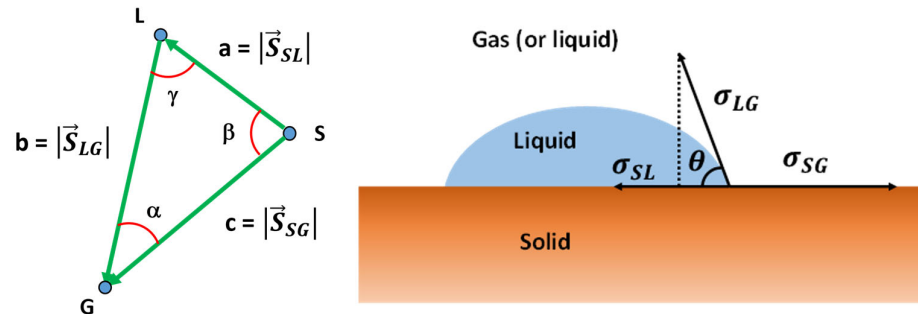


Figure 13. Angles between interaction vectors and contact angle.

Inside the Hansen field, the triangle formed by the interaction vectors that link solid, S, liquid, L, and gas, G, where the angles are  $\alpha, \beta, \gamma$ , and the sides opposite to these angles are  $a, b$ , and  $c$ , respectively, the opposite sides to the angles. The law of cosines is expressed as follows:

$$a^2 = b^2 + c^2 - 2bc \cdot \cos\alpha \tag{75}$$

Reorganizing:

$$c^2 - a^2 = 2bc \cdot \cos\alpha - b^2 \tag{76}$$

(72) can also be enunciated as follows:

$$\cos\theta = \frac{c^2 - a^2}{b^2} \tag{77}$$

Substituting (76) into (77) and operating, the following is obtained:

$$\cos\theta = 2 \frac{c}{b} \cdot \cos\alpha - 1 \tag{78}$$

$$\cos\theta = 2 \frac{\left| \vec{S}_{SG} \right|}{\left| \vec{S}_{LG} \right|} \cdot \cos\alpha - 1 \tag{79}$$

Figure 14 shows three relevant instances where the contact angle,  $\theta$ , and vectors are related.

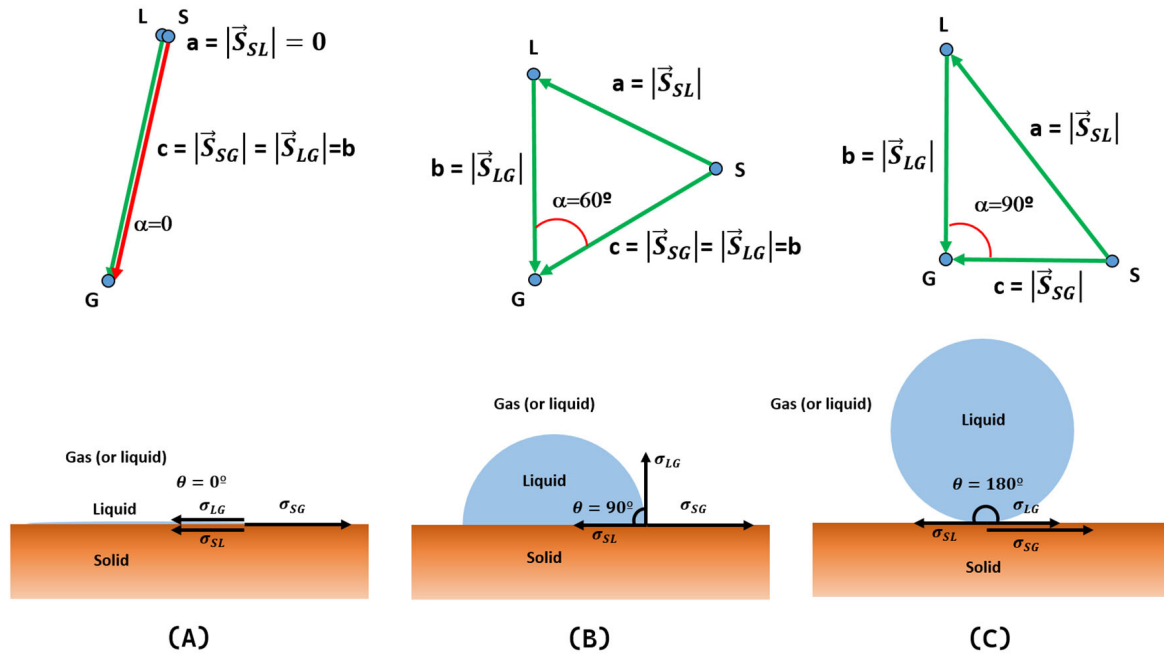


**Figure 14.** Relation between contact angle,  $\theta$ , and  $\alpha$  angle between  $\vec{S}_{SG}$  and  $\vec{S}_{LG}$  vectors. (A) maximum moisturizing, (B) intermediate moisturizing, and (C) zero moisturizing.

Case (a): Maximum moisturizing happens when  $\cos\theta = 1$ . In this situation:

$$\left| \vec{S}_{SG} \right| = \left| \vec{S}_{LG} \right| \quad \alpha = 0 \tag{80}$$

This means that maximum moisturization happens when the solid and liquid Hansen solubility parameters are the same because their vectors overlap each other.

Case (b): The contact angle is  $90^\circ$  when  $\cos\theta = 0$ , and this also implies the following:

$$\frac{\left| \vec{S}_{SG} \right|}{\left| \vec{S}_{LG} \right|} \cdot \cos\alpha = \frac{1}{2} \tag{81}$$

According to this expression, multiple configurations of  $\vec{S}_{SG}$  and  $\vec{S}_{LG}$  vectors, and the angles between them, are possible. One of the potential combinations is when  $\left| \vec{S}_{SG} \right| = \left| \vec{S}_{LG} \right|$  and  $\alpha = 60^\circ$ .

Case (c): Moisturizing is zero when  $\theta = 180^\circ$ , or, in other words,  $\cos\theta = -1$ . This happens when  $\vec{S}_{SG}$  and  $\vec{S}_{LG}$  vectors are perpendicular:  $\alpha = 90^\circ$ .

#### 4. Conclusions

The Hansen vector field model established in this paper allows us, among other things:

- (a) To link, for the first time, the cohesion energy of substances with their free surface energy, as surface or interfacial tension.
- (b) To calculate the surface tension and free energy of thousands of substances by knowing their Hansen solubility parameters, which are easily obtained from the molecular structure of substances. Likewise, it is possible to determine the interfacial tension between them with a simple vector calculation.
- (c) To theoretically calculate and accurately estimate contact angles that would, in many cases, be hard to experimentally determine. This vector field model saves experimental work and time.

Furthermore, this model allows us to empirically prove that the interface between two substances is not a mathematical surface with no thickness (as suggested by the Gibbs hypothesis), but indeed has a small-scale thickness, as proposed by Guggenheim. The said thickness is approximately half of the Bohr radius.

Further research is needed to explore the application of the Hansen vector space for other interactions such as polymer swelling, the chemical resistance of coatings, cracking, suspension stability, covering penetration, biological membrane penetration, absorption, adsorption, etc.

**Author Contributions:** Formal analysis, R.B.-M.; investigation, R.B.-M. and A.S.A.A.; methodology, R.B.-M. and A.S.A.A.; resources, R.B.-M. and A.S.A.A.; visualization, R.B.-M. and M.Á.B.-R.; writing—original draft, R.B.-M. and M.Á.B.-R.; writing—review and editing, R.B.-M., M.Á.B.-R. and A.S.A.A. All authors have read and agreed to the published version of the manuscript.

**Funding:** This research received no external funding.

**Institutional Review Board Statement:** This article does not contain any studies with human participants or animals performed by any authors.

**Informed Consent Statement:** Not applicable.

**Data Availability Statement:** The data that support the findings of this study will be available in the cited references.

**Acknowledgments:** This work has been carried out as part of the research of the doctoral thesis of Aqeel Shaikhah Arafat Aljadiri, directed by Rafael Bailón-Moreno. The doctoral thesis belongs to the Doctoral Program in Chemistry of the University of Granada (codes ISCED 1 Chemistry and ISCED 2 Physical, Chemical, Geological Sciences). Escuela Internacional de Postgrado of Universidad de Granada.

**Conflicts of Interest:** The authors declare no conflicts of interest.

## Appendix A

**Table A1.** Surface tension of liquids versus air,  $\sigma_{LG}$ , at 25 °C and solubility parameters. Medium and high-molar-volume and polar molecules in which the hydrogen bonding component is not relevant to surface tension.

N°	Substance	Ref.	$\sigma_{LG}$ , mN/m	$\delta_D$ , MPa <sup>1/2</sup>	$\delta_P$ , Mpa <sup>1/2</sup>	$\delta_H$ , MPa <sup>1/2</sup>	$4\delta_D^2 + \delta_P^2$ , MPa	$\sigma_{LG,cal.}$ , mN/m	Deviation, mN/m
1	1,1,2,2-Tetrabromoethane	2	48.9	22.6	5.1	8.2	2069.1	51.7	2.8
2	1,2,3-Tribromopropane	2	44.8	19.6	6.3	6.4	1576.3	39.4	−5.4
3	1,3-Diodopropane	2	46.3	19.4	5.7	4.3	1537.9	38.4	−7.9
4	1,4-Dioxane	2	32.3	19.0	1.8	7.4	1447.2	36.2	3.9
5	1-Bromonaphthalene	2	43.9	20.6	3.1	4.1	1707.1	42.7	−1.2
6	1-Butanol	1	24.7	16.0	5.7	15.8	1056.5	26.4	1.7
7	1-Chloro-2-Methylpropane	2	21.3	15.6	5.0	2.9	998.4	25.0	3.7
8	1-Chloro-3-Methylbutane	2	23.0	15.7	4.5	2.9	1006.2	25.2	2.2
9	1-Chlorobutane	2	22.5	16.2	5.5	2.0	1080.0	27.0	4.5
10	1-Chloronaphthalene	2	41.3	19.9	4.9	2.5	1608.1	40.2	−1.1
11	1-Decanol	2	28.1	16.0	4.7	10.0	1046.1	26.2	−1.9
12	1-Methyl Naphthalene	2	38.0	20.6	0.8	4.7	1698.1	42.5	4.5
13	1-Nitropropane	2	28.9	16.6	12.3	5.5	1253.5	31.3	2.4

Table A1. Cont.

N°	Substance	Ref.	$\sigma_{LG}$ , mN/m	$\delta_D$ , MPa <sup>1/2</sup>	$\delta_P$ , Mpa <sup>1/2</sup>	$\delta_H$ , MPa <sup>1/2</sup>	$4\delta_D^2 + \delta_P^2$ , MPa	$\sigma_{LG,cal.}$ , mN/m	Deviation, mN/m
14	1-Octanol	2	27.2	16.0	5.0	11.9	1049.0	26.2	−1.0
15	1-Propanol	2	23.7	16.0	6.8	17.4	1070.2	26.8	3.1
16	1-Propanol	1	27.5	16.0	6.8	17.4	1070.2	26.8	−0.7
17	2-Chloro-2-Methyl Propane	2	19.1	15.6	7.6	2.0	1031.2	25.8	6.7
18	2-Phenyl-ethanol	1	41.0	19.0	5.8	7.2	1477.6	36.9	−4.1
19	2-Propanol	2	22.6	15.8	6.1	16.4	1035.8	25.9	3.3
20	2-Propanol	1	27.0	15.8	6.1	16.4	1035.8	25.9	−1.1
21	3-Methylbutanenitrile	2	25.6	15.4	9.7	4.6	1042.7	26.1	0.5
22	Acetic acid	1	23.0	14.5	8.0	13.5	905.0	22.6	−0.4
23	Acetone	2	24.6	15.5	10.4	7.0	1069.2	26.7	2.1
24	Acetone	1	23.3	15.5	10.4	7.0	1069.2	26.7	3.4
25	Acetonitrile	1	28.6	15.3	18.0	15.8	1260.4	31.5	2.9
26	Aniline	2	43.1	19.4	5.1	10.2	1531.5	38.3	−4.8
27	Benzene	2	28.2	18.4	0.0	2.0	1354.2	33.9	5.7
28	Benzene	1	28.8	18.4	0.0	2.0	1354.2	33.9	5.1
29	Benzyl Alcohol	2	38.5	18.4	6.3	13.7	1393.9	34.8	−3.7
30	Benzyl Benzoate	2	45.4	20.0	5.1	5.2	1626.0	40.7	−4.7
31	Bromobenzene	2	35.9	19.2	5.5	4.1	1504.8	37.6	1.7
32	Bromoform	2	40.8	21.4	4.1	6.1	1848.7	46.2	5.4
33	Butanone	1	24.0	16.0	9.0	5.1	1105.0	27.6	3.6
34	Butyronitrile	2	27.6	15.3	12.4	5.1	1090.1	27.3	−0.3
35	Carbon Tetrachloride	2	26.3	16.1	8.3	0.0	1105.7	27.6	1.3
36	Chlorobenzene	2	33.0	19.0	4.3	2.0	1462.5	36.6	3.6
37	Chloroform	2	26.9	17.8	3.1	5.7	1277.0	31.9	5.0
38	Cis-Decahydronaphthalene	2	31.0	18.8	0.0	0.0	1413.8	35.3	4.3
39	Chloroform	1	27.2	17.8	3.1	5.7	1277.0	31.9	4.7
40	Cyclohexane	2	24.3	16.8	0.0	0.2	1129.0	28.2	3.9
41	Cyclohexane	1	28.8	16.8	0.0	0.2	1129.0	28.2	−0.6
42	Cyclohexanol	2	34.4	17.4	4.1	13.5	1227.9	30.7	−3.7
43	Cyclohexanone	1	28.2	16.8	5.7	8.0	1161.5	29.0	0.8
44	Cyclopentanol	2	32.2	17.2	5.3	12.8	1211.5	30.3	−1.9
45	Decane	2	23.4	15.7	0.0	0.0	986.0	24.6	1.2
46	Dichloromethane	1	27.0	17.0	7.3	7.1	1209.3	30.2	3.2
47	Dichloromethane	2	25.9	17.0	7.3	7.1	1209.3	30.2	4.3
48	Diethyl ether	1	18.6	14.5	2.9	5.1	849.4	21.2	2.6
49	Diethyl Fumarate	2	31.1	16.7	5.6	7.6	1146.9	28.7	−2.4
50	Diethyl Phthalate	2	36.7	17.6	9.6	4.5	1331.2	33.3	−3.4
51	Diiodomethane	2	50.1	22.0	3.9	5.5	1951.2	48.8	−1.3
52	Dimethyl Formamide	2	36.4	17.4	13.7	11.3	1398.7	35.0	−1.4
53	Dipropylene Glycol Monomethyl Ether	2	27.9	15.5	5.7	11.2	993.5	24.8	−3.1
54	Dodecane	2	24.9	16.0	0.0	0.0	1024.0	25.6	0.7
55	Ethanol	2	21.7	15.8	8.8	19.4	1076.0	26.9	5.2
56	Ethanol	1	21.6	15.8	8.8	19.4	1076.0	26.9	5.3
57	Ethyl 2-Aminobenzoate	2	39.0	18.7	8.3	7.9	1467.7	36.7	−2.3
58	Ethyl Acetate	1	24.9	15.8	5.3	7.2	1026.7	25.7	0.8
59	Ethyl Benzene	2	28.7	17.8	0.6	1.4	1267.7	31.7	3.0
60	Ethyl Bromide	2	23.6	16.5	8.4	2.3	1159.6	29.0	5.4
61	Ethylene Dichloride	2	32.6	19.0	7.4	4.1	1498.8	37.5	4.9
62	Ethylene Glycol Monoethyl Ether	2	28.1	16.2	9.2	14.3	1134.4	28.4	0.3
63	Furfural	2	41.3	18.6	14.9	5.1	1605.9	40.1	−1.2
64	Heptane	2	19.7	15.3	0.0	0.0	936.4	23.4	3.7
65	Hexachloro-1,3-Butadiene	2	35.5	19.1	5.3	0.6	1487.3	37.2	1.7
66	Hexadecane	2	27.0	16.3	0.0	0.0	1062.8	26.6	−0.4
67	Hexane	2	17.9	14.9	0.0	0.0	888.0	22.2	4.3
68	Iodobenzene	2	39.1	19.5	6.0	6.1	1557.0	38.9	−0.2
69	Isopropyl Benzene (Cumene)	2	27.7	18.1	1.2	1.2	1311.9	32.8	5.1
70	Limonene	1	26.4	17.2	1.8	4.3	1186.6	29.7	3.3
71	Mesitylene	2	28.4	18.0	0.0	0.6	1296.0	32.4	4.0
72	Methanol	2	22.3	15.1	12.3	22.3	1063.3	26.6	4.3
73	Methyl Anthranilate	2	43.7	19.1	8.9	8.7	1538.5	38.5	−5.2
74	Methyl Ethyl Ketone	2	24.0	16.0	9.0	5.1	1105.0	27.6	3.6
75	m-Nitrotoluene	2	40.8	18.9	7.3	4.0	1482.1	37.1	−3.7
76	m-Xylene	2	28.3	17.6	1.0	3.1	1240.0	31.0	2.7
77	N,N-Dimethyl Acetamide	2	36.0	16.8	11.5	9.4	1261.2	31.5	−4.5
78	n-Butyl acetate	1	27.8	15.8	3.7	6.3	1012.3	25.3	−2.5
79	n-Butylbenzene	2	28.7	17.4	0.1	1.1	1211.1	30.3	1.6
80	n-Heptane	1	19.7	15.3	0.0	0.0	936.4	23.4	3.7
81	Nitrobenzene	2	43.3	20.0	8.6	4.1	1674.0	41.8	−1.5
82	Nitroethane	2	31.3	16.0	15.5	4.5	1264.3	31.6	0.3
83	Nitromethane	2	36.0	15.8	18.8	6.1	1352.0	33.8	−2.2
84	N-Methyl-2-Pyrrolidone	2	40.2	18.0	12.3	7.2	1447.3	36.2	−4.0

Table A1. Cont.

N°	Substance	Ref.	$\sigma_{LG}$ , mN/m	$\delta_D$ , MPa <sup>1/2</sup>	$\delta_P$ , MPa <sup>1/2</sup>	$\delta_H$ , MPa <sup>1/2</sup>	$4\delta_D^2 + \delta_P^2$ , MPa	$\sigma_{LG,cal.}$ , mN/m	Deviation, mN/m
85	n-Tetradecane	2	26.1	16.2	0.0	0.0	1049.8	26.2	0.1
86	Octane	2	21.1	15.5	0.0	0.0	961.0	24.0	2.9
87	o-Nitrotoluene	2	40.9	19.0	7.5	4.3	1500.3	37.5	−3.4
88	o-Xylene	2	29.5	17.8	1.0	3.1	1268.4	31.7	2.2
89	p-Cymene	2	27.6	17.3	2.4	2.4	1202.9	30.1	2.5
90	Perfluoroheptane	2	12.4	12.0	0.0	0.0	576.0	14.4	2.0
91	Perfluorohexane (PFC 5060)	2	11.4	12.1	0.0	0.0	585.6	14.6	3.2
92	Perfluorooctane	2	13.5	12.1	0.8	0.3	586.3	14.7	1.2
93	Phenyl Isothiocyanate	2	40.9	19.4	13.9	8.5	1698.7	42.5	1.6
94	Propylbenzene	2	28.5	17.3	2.2	2.9	1202.0	30.1	1.6
95	Pyridine	2	37.3	19.0	8.8	5.9	1521.4	38.0	0.7
96	Pyrrrole	2	36.1	19.2	7.4	6.7	1529.3	38.2	2.1
97	Quinoline	2	42.6	19.8	5.6	5.7	1599.5	40.0	−2.6
98	Tetrachloroethylene	1	28.4	18.3	5.7	0.0	1372.1	34.3	5.9
99	Tetrahydrofuran	1	27.2	16.8	5.7	8.0	1161.5	29.0	1.8
100	Tetrahydrofuran	2	25.8	16.8	5.7	8.0	1161.5	29.0	3.2
101	Toluene	2	27.8	18.0	1.4	2.0	1298.0	32.4	4.6
102	Toluene	1	27.5	18.0	1.4	2.0	1298.0	32.4	4.9
103	Tricresyl Phosphate	2	40.5	19.0	12.3	4.5	1595.3	39.9	−0.6
104	Triethanolamine	5	45.9	17.3	22.4	23.3	1698.9	42.5	−3.4
105	Undecane	2	24.2	16.0	0.0	0.0	1024.0	25.6	1.4
106	Xylene (isomers)	1	27.8	17.7	1.0	3.1	1254.2	31.4	3.6

The “Ref” column indicates the origin of the surface tension data. When Ref is 1, it means that the data have been directly measured by the authors using the Harkins and Brown droplet weight method. When Ref is 2, it indicates that the data have been published by [10]. In some cases, surface tension data of the same substance, with Ref = 1 and Ref = 2 are shown in order to test the (always small) variability in both references. Moreover, the Hansen solubility parameters are included according to the values published in the second edition of his manual [5]. Likewise, the calculated squares of interaction vectors like  $4\delta_D^2 + \delta_P^2$ , the surface tensions calculated after linear regression and the absolute error between the calculated and experimental or bibliographic values are shown.

Table A2. Surface tension of liquids versus air,  $\sigma_{LG}$ , at 25 °C and solubility parameters. Low molar volume and high polar molecules.

N°	Substance	Ref.	$\sigma_{LG}$ , mN/m	$\delta_D$ , MPa <sup>1/2</sup>	$\delta_P$ , MPa <sup>1/2</sup>	$\delta_H$ , MPa <sup>1/2</sup>	$4\delta_D^2 + \delta_P^2 + \delta_H^2$ , MPa	$\sigma_{LG,cal.}$ , mN/m	Deviation, mN/m
107	1,5-Pentanediol	2	42.7	17.0	8.9	19.8	1627.3	40.7	−2.0
108	Diethylene Glycol	2	44.4	16.6	12.0	20.7	1674.7	41.9	−2.5
109	Diethylene Glycol	4	44.4	16.6	12.0	20.7	1674.7	41.9	−2.5
110	Dipropylene Glycol	2	33.4	16.5	10.6	17.7	1514.7	37.9	4.5
111	Dipropylene Glycol	1	34.8	16.5	10.6	17.7	1514.7	37.9	3.1
112	Dimethyl sulfoxide	1	42.2	18.4	16.4	10.2	1727.2	43.2	0.9
113	Dimethyl sulfoxide	3	41.8	18.4	16.4	10.2	1727.2	43.2	1.4
114	Dimethylformamide	3	39.1	17.4	13.7	11.3	1526.4	38.2	−0.9
115	Ethanolamine	2	48.3	17.0	15.5	21.2	1845.7	46.1	−2.2
116	Ethylene Glycol	2	47.3	17.0	11.0	26.0	1953.0	48.8	1.5
117	Formamide	2	57.8	17.2	26.2	19.0	2230.8	55.8	−2.0
118	Formic acid	3	31.4	14.3	11.9	16.6	1235.1	30.9	−0.5
119	Glycerol	2	64.3	17.4	12.1	29.3	2215.9	55.4	−8.9
120	Glycerol	3	63.7	17.4	12.1	29.3	2215.9	55.4	−8.3
121	3-Hydroxymethylpyridine	2	47.4	19.2	9.6	14.5	1777.0	44.4	−3.0
122	Water (molecule)	2	72.0	15.5	16.0	42.3	3006.3	75.2	3.2

When Ref is 1, it means that the surface tension values have been determined in a laboratory by the authors using the Harkins and Brown droplet weight method. The data with Ref = 2 are provided by [10], those with Ref = 3 are taken from [21], and those with Ref = 4 are from [22]. The solubility parameters data obtained by [5] are also shown. The calculated surface tension and absolute error with regard to the experimental or bibliographic values are also shown.

**Table A3.** Surface free energy of solids with air,  $\sigma_{LG}$ , at 25 °C and solubility parameters. Source: Weiyang Yu and Wanguo, 2019 [13].

N°	Substance	$\sigma_{SG}$ , mN/m	$\delta_D$ , MPa <sup>1/2</sup>	$\delta_P$ , MPa <sup>1/2</sup>	$\delta_H$ , MPa <sup>1/2</sup>	$4\delta_D^2 + \delta_P^2 + \delta_H^2$ , MPa	$\sigma_{SG,calc.}$ , mN/m	Deviation, mN/m
1	Polyethylene	33.0	17.3	1.7	2.1	1204.5	31.3	-1.7
2	Poly(vinyl chloride)	40.8	18.6	5.8	9.0	1498.5	39.0	-1.8
3	Poly(vinylidene chloride)	41.6	17.6	9.1	7.8	1382.7	35.9	-5.7
4	Poly(vinyl fluoride)	36.7	17.4	13.7	11.3	1526.4	39.7	3.0
5	Poly(vinylidene fluoride)	31.4	17.0	12.1	10.2	1406.5	36.6	5.2
6	Poly(tetrafluoroethylene)	15.0	15.1	0.9	1.7	915.7	23.8	8.8
7	Poly(ethylene terephthalate)	41.9	18.2	6.4	3.7	1379.6	35.9	-6.0
8	Poly(methyl methacrylate)	40.7	17.0	4.8	5.7	1211.5	31.5	-9.2
9	PA66	43.5	18.7	5.2	8.4	1496.4	38.9	-4.6
10	Polystyrene	41.3	20.5	3.1	2.6	1697.4	44.1	2.8
11	Polychlorotrifluoroethylene	26.9	14.1	2.7	5.5	832.8	21.7	-5.2
12	Polypropylene	30.1	18.1	1.0	0.0	1311.4	34.1	4.0
13	Polyisobutylene	33.6	16.9	2.5	4.0	1164.7	30.3	-3.3
14	Poly- $\alpha$ -methyl styrene	39.0	18.5	2.4	2.4	1380.5	35.9	-3.1
15	Poly-n-butyl methacrylate	31.2	15.9	5.5	5.9	1076.3	28.0	-3.2
16	Polycarbonate	34.2	18.4	5.9	6.9	1436.7	37.4	3.2
17	Polyethylmethacrylate	35.9	17.6	9.7	4.0	1349.1	35.1	-0.8
18	Graphite	35.0	18.0	9.3	7.7	1441.8	37.5	2.5
19	MoS <sub>2</sub>	34.4	18.0	9.0	6.2	1415.4	36.8	2.4
20	WS <sub>2</sub>	33.1	17.0	9.5	13.2	1420.5	36.9	3.8
21	BN	30.1	18.0	7.0	7.0	1394.0	36.2	6.1

**Table A4.** Interfacial tension of solids with liquids,  $\sigma_{SL}$ , at 25 °C and solubility parameters. Source: Masakazu Murase and Daisuke Nakamura, 2023 [10].

Solid	Liquid	HSP <sub>S</sub>					HSP <sub>L</sub>		$\left  \vec{S}_{SL} \right ^2$ , MPa	$\sigma_{SL,calc.}$ , mN/m	Deviation, mN/m
		$\sigma_{SL}$ , mN/m	$\delta_{DS}$ , MPa <sup>1/2</sup>	$\delta_{PS}$ , MPa <sup>1/2</sup>	$\delta_{HS}$ , MPa <sup>1/2</sup>	$\delta_{DL}$ , MPa <sup>1/2</sup>	$\delta_{PL}$ , MPa <sup>1/2</sup>	$\delta_{HL}$ , MPa <sup>1/2</sup>			
PS	Water	49.4	20.6	2.5	1.5	15.5	16.0	42.3	1953.8	52.8	3.4
	Formamide	26.6	20.6	2.5	1.5	17.2	26.2	19.0	914.2	24.7	-1.9
	Ethylene Glycol	21.9	20.6	2.5	1.5	17.0	11.0	26.0	726.0	19.6	-2.3
	Benzyl Alcohol	0.4	20.6	2.5	1.5	18.4	6.3	13.7	183.5	5.0	4.6
	Nitromethane	8.1	20.6	2.5	1.5	15.8	18.8	5.1	369.8	10.0	1.9
PMMA	Water	27.0	18.5	9.0	8.4	15.5	16.0	42.3	1235.6	33.4	6.4
	Formamide	17.2	18.5	9.0	8.4	17.2	26.2	19.0	414.1	11.2	-6.0
	Ethylene Glycol	17.9	18.5	9.0	8.4	17.0	11.0	26.0	323.7	8.7	-9.2
	Benzyl Alcohol	5.3	18.5	9.0	8.4	18.4	6.3	13.7	36.0	1.0	-4.3
	1-Bromonaphtalene	3.9	18.5	9.0	8.4	20.6	3.1	4.1	71.6	1.9	-2.0
Nitromethane	8.7	18.5	9.0	8.4	15.8	18.8	5.1	134.4	3.6	-5.1	
PA66	Water	15.6	19.5	6.2	14.7	15.5	16.0	42.3	921.3	24.9	9.3
	Formamide	9.6	19.5	6.2	14.7	17.2	26.2	19.0	438.6	11.8	2.2
	Ethylene Glycol	10.4	19.5	6.2	14.7	17.0	11.0	26.0	175.4	4.7	-5.7
	Benzyl Alcohol	6.0	19.5	6.2	14.7	18.4	6.3	13.7	5.7	0.2	-5.8
	1-Bromonaphtalene	1.7	19.5	6.2	14.7	20.6	3.1	4.1	126.9	3.4	1.7
Nitromethane	9.9	19.5	6.2	14.7	15.8	18.8	5.1	304.4	8.2	-1.7	
PTFE	Water	55.8	13.6	1.7	0.0	15.5	16.0	42.3	2008.4	54.2	-1.6
	Formamide	31.1	13.6	1.7	0.0	17.2	26.2	19.0	1013.6	27.4	-3.7
	Ethylene Glycol	27.2	13.6	1.7	0.0	17.0	11.0	26.0	809.7	21.9	-5.3
	Benzyl Alcohol	13.6	13.6	1.7	0.0	18.4	6.3	13.7	302.8	8.2	-5.4
	1-Bromonaphtalene	13.8	13.6	1.7	0.0	20.6	3.1	4.1	217.5	5.9	-7.9
	Nitromethane	8.1	13.6	1.7	0.0	15.8	18.8	5.1	338.0	9.1	1.0
	n-Decane	2.9	13.6	1.7	0.0	15.7	0.0	0.0	21.4	0.6	-2.3
	n-Hexane	2.7	13.6	1.7	0.0	14.9	0.0	0.0	10.2	0.3	-2.4
Dimethyl sulfoxide	15.0	13.6	1.7	0.0	18.4	16.4	10.2	413.6	11.2	-3.8	
PVB	Water	33.9	17.9	8.3	4.2	15.5	16.0	42.3	1534.2	41.4	7.5
	Formamide	18.3	17.9	8.3	4.2	17.2	26.2	19.0	540.9	14.6	-3.7
	Ethylene Glycol	20.0	17.9	8.3	4.2	17.0	11.0	26.0	486.0	13.1	-6.9
	Benzyl Alcohol	8.4	17.9	8.3	4.2	18.4	6.3	13.7	95.6	2.6	-5.8
	1-Bromonaphtalene	3.0	17.9	8.3	4.2	20.6	3.1	4.1	56.6	1.5	-1.5
Nitromethane	9.1	17.9	8.3	4.2	15.8	18.8	5.1	128.1	3.5	-5.6	

**Table A5.** Contact angle of diverse liquids over PMMA and n-Octacosane. PMMA solubility parameters:  $\delta_D = 18.64$ ,  $\delta_P = 10.52$ ,  $\delta_H = 7.51$ . n-Octacosane solubility parameters:  $\delta_D = 16.91$ ,  $\delta_P = 0$ ,  $\delta_H = 0$ . Source: J. Panzer, 1973 [14].

Liquid	Solid	$\theta_{exp.}$	$\delta_D$ , MPa <sup>1/2</sup>	$\delta_P$ , MPa <sup>1/2</sup>	$\delta_H$ , MPa <sup>1/2</sup>	$\left  \vec{S}_{LG} \right ^2$	$\left  \vec{S}_{SG} \right ^2$	$\left  \vec{S}_{SL} \right ^2$	$\theta_{calc.}$
Octane	n-Octacosane	0	15.5	0.0	0.0	961.0	1143.8	8.0	0
2-Propanol	PMMA	0	15.8	6.1	16.4	1035.8	1556.9	130.8	0
Acetone	PMMA	0	15.5	10.4	7.0	1069.2	1556.9	39.7	0
Benzyl alcohol	PMMA	0	18.4	6.3	13.7	1393.9	1556.9	56.4	0
Bromobenzene	PMMA	0	19.2	5.5	4.1	1504.8	1556.9	38.1	0
Ethyl acetate	PMMA	0	15.8	5.3	7.2	1026.7	1556.9	59.6	0
Octane	PMMA	0	15.5	0.0	0.0	961.0	1556.9	206.5	0
Tetrahydrofuran	PMMA	0	16.8	5.7	8.0	1161.5	1556.9	37.0	0
Chlorobenzene	PMMA	1	19.0	4.3	2.0	1462.5	1556.9	69.6	0
Dodecane	PMMA	1	16.0	0.0	0.0	1024.0	1556.9	194.9	0
Pyridine	PMMA	1	19.0	8.8	5.9	1521.4	1556.9	6.1	0
Ethanol	PMMA	2.5	15.8	8.8	19.4	1076.0	1556.9	176.6	0
Methanol	PMMA	3	15.1	12.3	22.3	1063.3	1556.9	272.0	0
o-xylene	PMMA	3	17.8	1.0	3.1	1268.4	1556.9	112.9	0
Hexadecane	PMMA	4	16.3	0.0	0.0	1062.8	1556.9	189.0	0
Nitroethane	PMMA	7	16.0	15.5	4.5	1264.3	1556.9	61.7	0
Carbon Tetrachloride	PMMA	8	16.1	8.3	0.0	1105.7	1556.9	87.1	0
Cyclohexanol	PMMA	8	17.4	4.1	13.5	1227.9	1556.9	83.2	0
Carbon Tetrachloride	n-Octacosane	24	17.8	0.0	0.6	1267.4	1143.8	3.5	26
Diethylene glycol	PMMA	35	16.6	12.0	20.7	1674.7	1556.9	192.8	35
Cyclohexanol	n-Octacosane	36	17.4	4.1	13.5	1227.9	1143.8	200.0	40
Bromoform	n-Octacosane	39	21.4	4.1	6.1	1848.7	1143.8	134.7	57
Pyridine	n-Octacosane	39	19.0	8.8	5.9	1521.4	1143.8	129.7	48
Nitroethane	n-Octacosane	40	16.0	15.5	4.5	1264.3	1143.8	263.8	46
Nitrobenzene	n-Octacosane	45	20.0	8.6	4.1	1674.0	1143.8	129.0	53
Nitromethane	n-Octacosane	51	15.8	18.8	6.1	1352.0	1143.8	395.6	56
Ethylene Glycol	PMMA	51	17.0	11.0	26.0	1953.0	1556.9	352.9	52
Formamide	PMMA	52	17.2	26.2	19.0	2230.8	1556.9	386.2	58
Glycerol	PMMA	68	17.4	12.1	29.3	2215.9	1556.9	483.5	61
Water	PMMA	71	15.5	16.0	30.3	2135.1	1556.9	588.9	63
Diethylene glycol	n-Octacosane	76	16.6	12.0	20.7	1674.7	1143.8	572.9	70
Dimethyl sulfoxide	n-Octacosane	76	18.4	16.4	10.2	1727.2	1143.8	381.9	64
Ethylene Glycol	n-Octacosane	86	17.0	11.0	26.0	1953.0	1143.8	797.0	80
Formamide	n-Octacosane	95	17.2	26.2	19.0	2230.8	1143.8	1047.8	88
Glycerol	n-Octacosane	95	17.4	12.1	29.3	2215.9	1143.8	1005.9	86
Water	n-Octacosane	106	15.5	16.0	30.3	2135.1	1143.8	1182.0	91

The solubility parameters values from liquids and Poly(methyl methacrylate) (PMMA) are the ones published by [5]. The n-Octacosane solubility parameters have been calculated by extrapolating the homologue hydrocarbons data published by Hansen also. The square of the module of the interaction vector for liquid–air, solid–air and solid–liquid interactions and the calculated contact angle data are also shown in the table.

## References

1. Elliot, J.A.W. Gibbsian Surface Thermodynamics. *J. Phys. Chem. B* **2020**, *124*, 10859–10878. [[CrossRef](#)] [[PubMed](#)]
2. Kirkwood, J.G.; Buff, F.P. The Statistical Mechanical Theory of Surface Tension. *J. Chem. Phys.* **1949**, *17*, 338–343. [[CrossRef](#)]
3. Yu, Y.X. A novel weighted density functional theory for adsorption, fluid–solid interfacial tension, and disjoining properties of simple liquid films on planar solid surfaces. *J. Chem. Phys.* **2009**, *131*, 024704. [[CrossRef](#)] [[PubMed](#)]
4. Hildebrand, J.H.; Scott, R.L. *The Solubility of Nonelectrolytes*; Reinhold: New York, NY, USA, 1950.
5. Hansen, C.M. *Hansen Solubility Parameters. A User's Handbook*; CRC Press, Taylor & Francis Group: Boca Raton, FL, USA, 2007.
6. Beerbower, A. Surface Free Energy: A New Relationship to Bulk Energies. *J. Colloid Interface Sci.* **1971**, *35*, 126–131. [[CrossRef](#)]
7. Koenhen, D.M.; Smolders, C.A. The determination of Solubility Parameters of Solvents and Polymers by Means of Correlations with other Physical Quantities. *J. Appl. Polym. Sci.* **1975**, *19*, 1163–1179. [[CrossRef](#)]
8. Large, M.J.; Ogilvie, S.P.; King, A.A.K.; Dalton, A.B. Understanding Solvent Spreading for Langmuir Deposition of Nanomaterial Films: A Hansen Solubility Parameter Approach. *Langmuir* **2017**, *33*, 14766–14771. [[CrossRef](#)] [[PubMed](#)]
9. AlQasas, N.; Eskhan, A.; Johnson, D. Hansen Solubility Parameters from Surface Measurements: A Comparison of Different Methods. *Surf. Interfaces* **2023**, *36*, 102594. [[CrossRef](#)]
10. Murase, M.; Nakamura, D. Hansen Solubility Parameters for Directly Dealing with Surface and Interfacial Phenomena. *Langmuir* **2023**, *39*, 10475–10484. [[CrossRef](#)] [[PubMed](#)]

11. Abbott, S.; Hansen, C.M.; Yamamoto, H.; Valpey, R.S. *Hansen Solubility Parameters in Practice, Complete with eBook, Software and Data*; Hansen-Solubility: Hørsholm, Denmark, 2013.
12. Harkins, W.D.; Brown, F.E. The Determination of Surface Tension (Free Surface Energy) and the Weight of Falling Drops: The Surface Tension of Water and Benzene by the Capillary Method. *J. Am. Chem. Soc.* **1919**, *41*, 499–525. [[CrossRef](#)]
13. Yu, W.; Hou, W. Correlations of Surface Free Energy and Solubility Parameters for Solid Substances. *J. Colloid Interface Sci.* **2019**, *544*, 8–13. [[CrossRef](#)] [[PubMed](#)]
14. Panzer, J. Components of Solid Surface Free Energy from Wetting Measurements. *J. Colloid Interface Sci.* **1973**, *44*, 142–161. [[CrossRef](#)]
15. Gibbs, J.W. On the equilibrium of heterogeneous substances. *Am. J. Sci.* **1878**, *s3–s16*, 441–458. [[CrossRef](#)]
16. Guggenheim, E.A. The Thermodynamics of Interfaces in Systems of Several Components. *Trans. Faraday Soc.* **1940**, *35*, 397–411. [[CrossRef](#)]
17. Dadashev, R.K.; Elimkhanov, D.Z.; Kutuev, R.A.; Umarhadzhev, K.S. Concentration Dependence of the Distance Between Different Positions of the Gibbs Dividing Surface in Two-Component Solutions. *Russ. J. Phys. Chem. A* **2021**, *95*, 2290–2294. [[CrossRef](#)]
18. Cho, J. Pressure Coefficient of Interfacial Tension for Polymer Blends. *Macromol. Res.* **2013**, *21*, 1360–1365. [[CrossRef](#)]
19. Cho, J. Superposition in Flory-Huggins  $\chi$  and Interfacial Tension for Compressible Polymer Blends. *Macro Lett.* **2013**, *2*, 544–549. [[CrossRef](#)] [[PubMed](#)]
20. Werner, A.; Schmid, F.; Müller, M.; Binder, K. “Intrinsic” Profiles and Capillary Waves at Homopolymer Interfaces: A Monte Carlo Study. *Phys. Rev. E* **1999**, *59*, 728–738. [[CrossRef](#)]
21. Singh, M. Survisometer, 2-in-1 For Viscosity and Surface Tension Measurement, an Excellent Invention for Industrial Proliferation of Surface Forces in Liquids. *Surf. Rev. Lett.* **2007**, *14*, 973–983. [[CrossRef](#)]
22. Gaur, A.P.S.; Sahoo, S.; Ahmadi, M.; Dash, S.P.; Guinel, M.J.-F.; Katiyar, R.S. Surface Energy Engineering for Tunable Wettability through Controlled Synthesis of MoS<sub>2</sub>. *Nano Lett.* **2014**, *14*, 4314–4321. [[CrossRef](#)] [[PubMed](#)]

**Disclaimer/Publisher’s Note:** The statements, opinions and data contained in all publications are solely those of the individual author(s) and contributor(s) and not of MDPI and/or the editor(s). MDPI and/or the editor(s) disclaim responsibility for any injury to people or property resulting from any ideas, methods, instructions or products referred to in the content.